ALMA MATER STUDIORUM – UNIVERSITÀ DI BOLOGNA

SCUOLA DI INGEGNERIA E ARCHITETTURA

CORSO DI LAUREA MAGISTRALE IN CIVIL ENGINEERING

DIPARTIMENTO DI INGEGNERIA CIVILE, AMBIENTALE E DEI MATERIALI

TESI DI LAUREA

in

Advanced Hydrosystems Engineering

TOXICITY EVALUATION OF TiO2 NANOPARTICLES EMBEDDED IN CONSUMER PRODUCTS

CANDIDATO

Andrea Galletti

RELATORE:

Chiar.mo Prof. Andrea Bolognesi

CORRELATORE:

Prof. Sung Hee Joo

Anno Accademico 2015/2016

Sessione I

Keywords

Titanium Dioxide

Personal Care Products

Toxicity

Diatom

TABLE OF CONTENTS

Abstract

Lo studio è orientato alla determinazione dei rischi tossici posti dalle nanoparticelle di diossido di titanio rilasciate in ambiente marino. L'organismo modello utilizzato per questo studio è la diatomea *Thalassiosira pseudonana*, la quale è stata scelta per la sua semplicità biologica unita alla fondamentale rilevanza nella catena alimentare e nell'ecosistema marino.

Oltre alle nanoparticelle prodotte industrialmente, questo studio ha lo scopo di determinare e confrontare la tossicità delle nanoparticelle utilizzate in alcuni prodotti di cura personale (in particolare crema solare e dentifricio), estraendole direttamente da essi.

I nostri risultati mostrano una notevole ridondanza nel legame tra la natura (il tipo) delle nanoparticelle e l'inibizione della normale crescita delle diatomee, che supera la correlazione con tutti gli altri parametri monitorati (concentrazione di nanoparticelle, tempo di esposizione, pH, carica superficiale e dimensione delle particelle stesse), sebbene gli altri parametri risultino direttamente legati agli effetti inibitori.

Tali risultati suggeriscono un'intensificazione della ricerca nell'ambito delle nanotecnologie, orientata allo sviluppo di nanomateriali "sostenibili", ovvero dei quali sono note le potenzialità di impiego, ma anche gli aspetti negativi, che possono di conseguenza essere monitorati con maggiore consapevolezza.

Chapter 1 – Introduction

In recent years, metal oxide nanoparticles (MONPs) have experienced a growing trend in their use in a wide range of industrial applications. Among them, titanium dioxide nanoparticles (commonly referred to as nano-TiO_2 or TiO_2 NPs) are by far the most used, in industry, agriculture, personal care products (PCPs, including but not limited to, cosmetics, sunscreens, and toothpaste), electronics, food dressing, and food packaging. The main properties TiO_2 NPs are their whiteness and opacity, along with some known antibacterial effects. Different studies have tried to estimate the production rate of nano-TiO_2, and how it is distributed among its different fields of application.

Piccinno et al. (2012)[1] surveyed 18 producers of nano-TiO_2, assessing the top usage of TiO_2 in the field of PCPs, standing at 68% of the total produced nano-TiO_2. As it can be seen from Figure 1.1, other relevant fields of application for TiO_2 NPs are plastics (6%), paints (14%), and other applications (e.g., cement) (12%). In the same study, the globally produced TiO_2 NPs is reported to be on average 3,000 tons per year, in a range of 101 to 10,000 (5% and 95% confidence limits), based on a 56% response rate (10 producers out of 18).

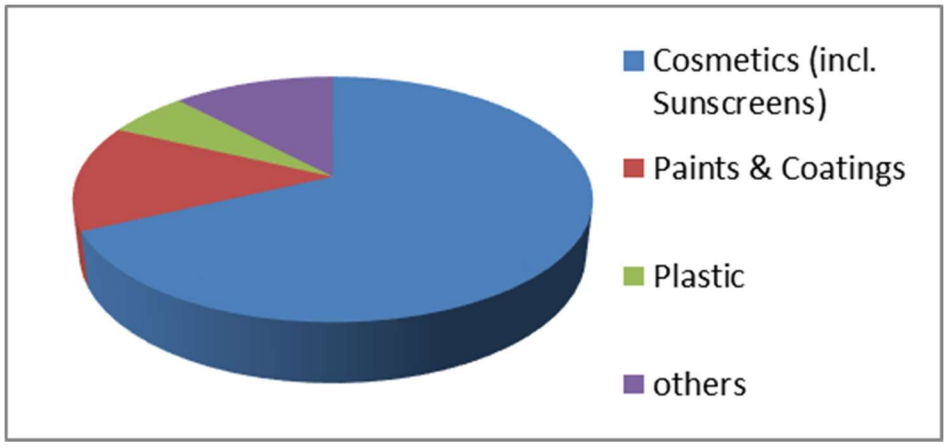

Figure 1.1. Main applications of Titanium Dioxide nanoparticles in industry.[1]

Another study[2] predicted that most of the currently produced TiO_2 will be converted into nano-TiO_2 by the end of year 2026, reaching an overall production rate of 2.5 million tons per year. As it can be observed from figure 1.2., nanoscale

TiO_2 will replace the bulk scale material at an exponentially increasing rate, substituting it completely by the end of year 2026.

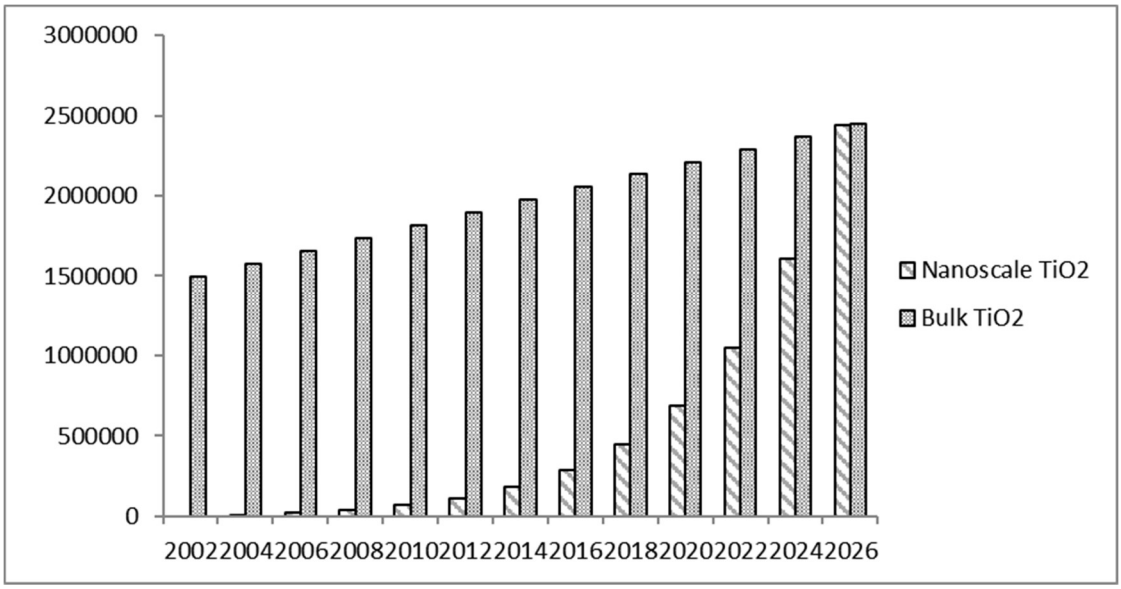

Figure 1.2. Prediction of the demand of Titanium Dioxide for industrial applications.[2]

A study from Lewicka Z. et al. (2011)[3] reported that the TiO_2-NPs used in commercial sunscreens exhibit the rutile crystalline structure rather than the anatase crystalline structure (which is dominant in the industrially produced TiO_2-NPs). TiO_2 NPs are mostly needle or near-spherically-shaped, having a size generally lower than 20 nm and are often coated with silica or alumina. However, despite the large production and usage of TiO2-NPs, little is known about their potential effects on health and the environment.

Chang X. et al. (2013)[4] reviewed all the available studies concerning TiO_2-NPs toxicity to the human body. The selected articles (347 in total) were all related to particles smaller than 100 nm (i.e., nanoparticles), clearly stated the target cell or organism (either human or animal) and the experimental exposure conditions. Their findings highlighted the presence of nano-TiO_2 in various important organs, such as liver, kidney, spleen and brain.

Wang S. et al., (2013)[5] investigated the effect of nano-TiO_2 exposure in mice, finding out that nanoparticles absorbed by adults were transmitted to their offsprings during pregnancy, leading to the presence of NPs in their brain and testes causing

decreased sperm production, along with other effects. In addition to its potential genotoxic effects, exposure to nano-TiO_2 was also shown by Sun H. et al. (2007)[6] to increase the mortality of carp.

Regarding nano-TiO_2 interaction with UV radiation, several studies[7–9] highlighted the photo-activity of nano-TiO2: when irradiated with solar light, nano-TiO_2 was shown to increase the mortality of several viruses, bacteria, organic and inorganic contaminants more than without UV irradiation; nano-TiO_2 photo-toxicity is mainly exerted through the production of ROS (reactive oxygen species) which may cause endocrine disruption. Furthermore, TiO_2 NPs were shown to have antimicrobial properties.[9,10]

Considering the increasing trend in the use of nano-TiO_2 for an ever-increasing range of applications and products, the occurrence of accumulation-related environmental events is likely, as much as their release and accumulation into the ecosystem, both fluvial and marine. However, to the current state of knowledge, no long term data on the potential hazards posed by nano-TiO_2 pollution are available, due to the relative newness of this technology. Given the significant production and consequent release of nanoparticles to the aquatic environment, the ecosystem might incur dangerous modifications, with detrimental impacts on its organisms. Nonetheless, release of TiO_2 NPs to water bodies might ultimately result in its accumulation in drinking water.[11]

Further concerns are posed for environmental systems in which a variety of pollutants are present. Due to its chemical and physical properties, nano-TiO_2 can effectively adsorb and transport other substances on its surface, easing their accumulation in different end-points. As an example, a study conducted by Hartmann N. B. et al. (2012)[12] showed that cadmium metal strongly adsorbs onto nano-TiO_2 surface due to the nanoparticles' small size, large surface area, and strong electronic attraction. After being transported, cadmium was found to accumulate into various marine organisms with an increased uptake but without influencing its bioavailability to the tested organisms.

The goal of this study is to investigate the significance of toxicity of nano-TiO_2 released by PCPs towards marine algae, and to compare it to industrially-produced TiO_2 NPs. Two different commercialized PCPs will be investigated (sunscreen and toothpaste), in accordance with the study`s aim. The toxicological results will hopefully provide more insight into the subject of nano-pollution of the marine environment, as well as a starting point for future investigation.

Chapter 2 - Literature review

Titanium dioxide is one of the most widely spread nano metal oxides in a variety of industrial applications. Due to its macroscopic characteristics of whiteness and opacity, it is used in many personal care products (including sunscreen and toothpaste), paintings and covers, whitening of foods and paper, etc. Nano-TiO_2 has an open cycle, meaning that at the end of its useful life it is released almost entirely into the environment, through different routes.[1] As can be observed from Figure 2.1., Nano-TiO_2 is the second most produced nano metal oxide worldwide, for a total of 3000 tons every year. The world-wide produced amounts of other relevant metal oxide nanoparticles are summarized in Table 2.1.

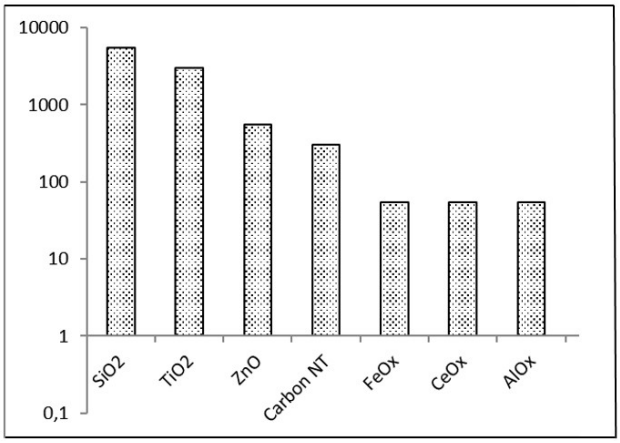

Figure 2.1. Worldwide production of Metal Oxide nanoparticles in tons/year.[1]

Table 2.1. Worldwide produced amounts of Metal Oxide nanoparticles (tons/year). [1]

MO-NP	**tons/y**
SiO_2	5500
TiO_2	3000
ZnO	550
CNT	300
FeOx	55
CeOx	55
AlOx	55

Yin T. et al. (2014)[13] developed a probabilistic emission model for five industrially used engineered nanoparticles (TiO_2, ZnO, Ag, CNT, and fullerenes), basing the model on the available information from producers and retailers in Europe (with a focus on Switzerland). The lifecycle flow charts were complemented with quantitative information retrieved from different companies in order to determine the final percentage of material released to the environment. According to the available data, different probability distributions were developed; in particular, as can be seen from Figure 2.2, nano-TiO_2 production was modeled yielding a resulting mode 10,000 tons/year, making it the engineered nanoparticle with the highest production.

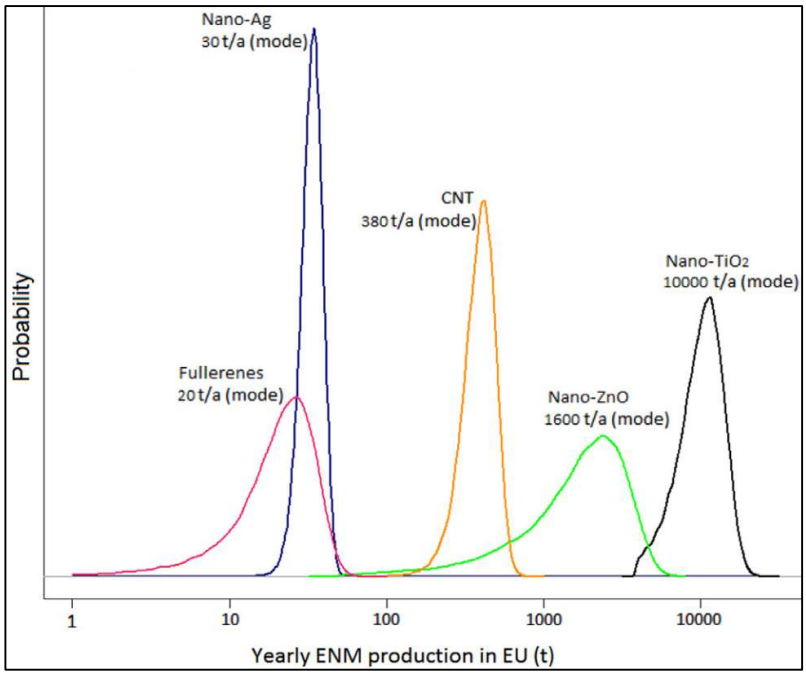

Figure 2.2. Probabilistic distribution for various ENPs' yearly production in Europe.[13]

Moreover, data were taken into account following the probabilistic approach named Degree of Belief, based on the precision and accuracy of each datum. In this way it was possible to model the intrinsic variability involved in the lifecycle of a nanoparticle via Monte Carlo simulation, managing to deal with sources of uncertainty in a uniform way.

Uncertainty parameters were related to different steps of the products' lifecycle, such as production, distribution, and especially use and disposal, which determine

the highest share of release of nanoparticles to the environment. The same study also developed mass-flow logic diagrams for the five engineered nanoparticles on a European scale, eventually providing stepping stone for future development or for the regulation of emissions. Mass-flow diagrams concerning nano-TiO_2 are shown in Figure 2.3. A similar study should be conducted on a worldwide scale, to better understand the emission trend the environment is going to face in the upcoming years.

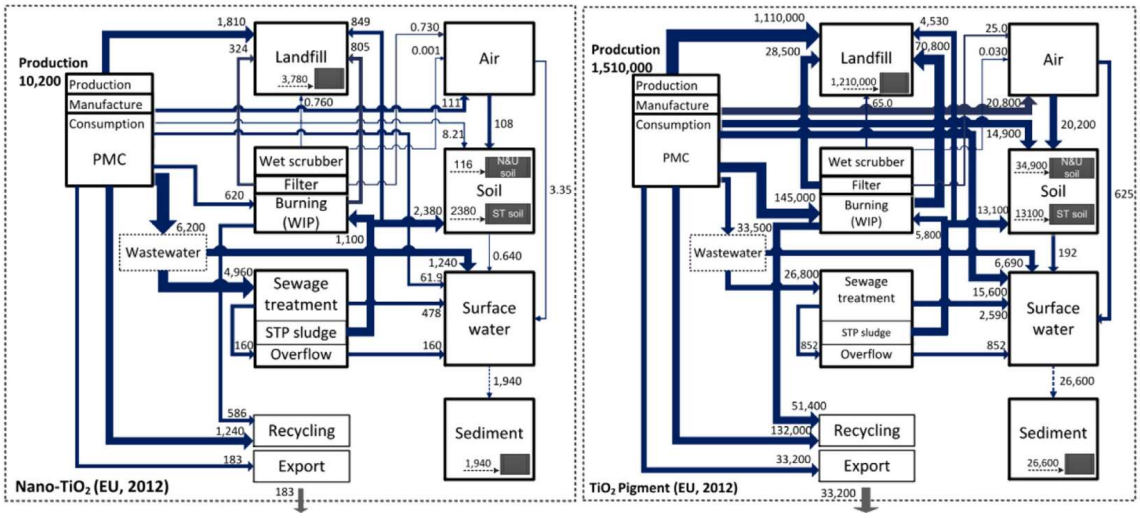

Figure 2.3. Mass-flow logic diagram for Nano TiO2 and TiO2 Pigment on a EU scale.[13]

A study from Weir et al. (2012)[14] investigated the presence of nano-TiO_2 in a range of personal care products, pharmaceuticals, foods, deodorants, as well as in other products known to make use of TiO_2 NPs. From the analysis of eight different toothpastes, the titanium content ranged from 0.7 to 5.6 mg/g-product, meaning from less than 0.1% to more than 0.5% in weight. All the findings were consistent with what was reported on labels. In the same study, a similar analysis conducted on three different sunscreens revealed a much higher content of TiO_2, measured between 14 and 90 mg/g-product (1.4% to 9% in weight). Among the tested products, sunscreens were by far the ones with the highest content of nano-TiO_2. Since sunscreens are directly washed off into the marine environment (when they are not completely absorbed into skin), this result poses a fundamental threat to the marine ecosystem.

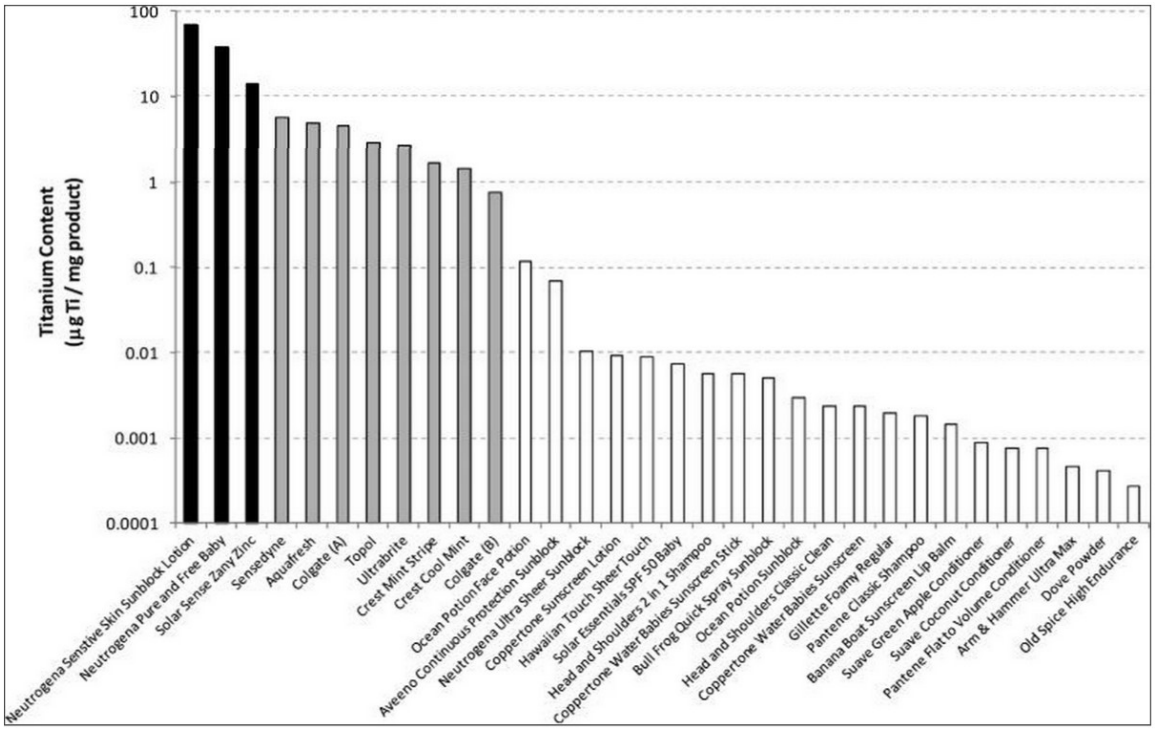

Figure 2.4. Titanium Dioxide Nanoparticles content in sunscreens (black), toothpastes (grey), and other personal care products (white) expressed in parts-per-thousand.[14]

The physical properties of TiO_2 NPs used in different commercial sunscreens were investigated by Lewicka Z. et al. (2011)[3] through different techniques, including XRD, SEM and TEM observation, and BET surface area analysis. From their findings, eight sunscreens use nano-TiO_2 in the rutile crystalline structure and only one presented nano-TiO2 in the anatase crystalline structure. Particles were needle or near spherically-shaped and measured around 25 nm in their primary particle size. In their experiments Clément et al. (2013)[15], analyzed the correlation between crystalline structure and particle size of both anatase and rutile form nano-TiO_2 and its toxicity to marine organisms using rotifers, algae, and daphnies as model organisms. As a result, they discovered that anatase form nanoTiO_2 is toxic in all of the performed toxicity tests (acute, medium acute and long term); whereas rutile nanoTiO_2 tends to form large agglomerates while in aqueous suspension, thus becoming a minor threat in terms of toxicity. It was also demonstrated that exposure time, particle aggregation, and concentration are contributing factors in nanoparticle-mediated toxicity. Further analyses on the non-volatile inorganic residuals revealed

the presence of other nano metal oxides (Al_2O_3 and SiO_2) used as coating agents for TiO_2 NPs, in order to reduce its photo-activity.[3]

Another study from Lewicka Z. et al. (2013)[16] investigated the possible ROS (Reactive Oxygen Species) production upon UVA and UVB irradiation for eight different commercial sunscreens, through quantitative measurements. TiO_2 NPs ROS production proved to be negligible, due to the effectiveness of the coating materials (silica and alumina) used to minimize their photo-activity. However, a similar study conducted by Rincon et al. (2004)[17] demonstrated how water solar disinfection through ROS production by means of nano-TiO_2 is an effective process. Additionally, Kwak S. Y. et al. (2001)[18] found application for TiO_2 antibacterial properties in membrane filters: a nano-TiO_2-based membrane was fouled by *E. coli* less than a traditional one when irradiated with UV.

Rincon's experimental procedure[17] planned to irradiate various bacteria (coliforms and cocci) with UV radiation, and to repeat the same treatment with the addition of TiO_2 to the cultures. As a result, the sole UV irradiation did not prevent a normal bacterial growth; however, the addition of TiO_2 NPs caused a decrease in the population count, even after terminating the irradiation process for the following 60 hours. ROS production is by far the most credited toxicity mechanism among metal oxide NPs, yet the real link between metal oxide NPs and ROS production remains ambiguous. ROS exist in different forms with slightly different toxicity mechanisms (e.g., OH- radicals, hydrogen peroxide in combination with other ROS, superoxide ions). ROS production is due mainly to UV light, although in some cases visible light can also contribute (e.g., ZnO, which has a large band gap). At a molecular level, ROS production seems to be due to oxygen vacancies in the NP. The mechanisms involved in nano-TiO_2 photo-toxicity need, therefore, to undergo further investigation in order to assess the risks posed by the nanomaterial.

Many studies on the possible genotoxicity caused by exposure to TiO_2 NPs were reviewed by Chen T. et al. (2013)[19], who found that TiO_2 NPs under UV radiation may cause modifications in the DNA leading to cell mutation diseases (e.g., cancer). However, results are not unique among the existing studies. The review included a

variety of studies on in vivo and in vitro tests, on different organisms: tests on human lymphocytes, bronchial and lung cells yielded either positive or negative results, as well as studies conducted on hamsters and mice exposed to inhalation of nano-TiO_2. In vivo mutation tests were conducted on mice and on *Drosophila Melanogaster*, but still did not yield uniform results, thus urging us toward a deeper understanding of this phenomenon.

As for marine environment eco-toxicity, the available studies have been reviewed by Minetto D. et al. (2014)[20] who found that the cell growth inhibition test was the only kind of test used to assess nano-TiO_2 eco-toxicity. Species that have already been tested for nanoTiO_2 toxicity are *Dunaliella tertiolecta, Isochrysis galbana, Phaeodactylum tricornutum, Thalassiosira pseudonana* and *Skeletonema*. From the overall results of past studies, it appears still difficult to establish whether nanoTiO_2 is toxic to the marine environment or not, as different species derived different results. Also, tests were performed under non standardized environmental conditions, thus making their results inconsistent with other literature. The works reviewed by Minetto et al. are synthesized in Figure 2.5 and highlight the relatively low amount of studies on nanoparticles' toxicity in the marine environment, as of 2014.

A review of toxicity tests for different metal oxide nanoparticles on marine

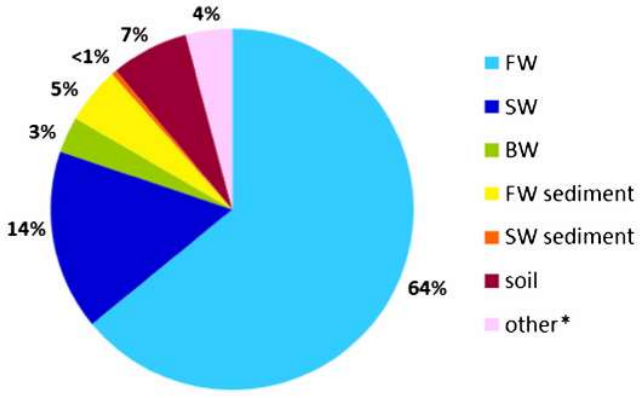

Figure 2.5. Studies reviewed by Minetto et al. (2014) regarding nanoparticles' toxicity in water environment, subdivided between freshwater, sea water and brackish water. [20]

species is shown in Table 2.3.

Miller et al. (2012)[21] performed an inhibition test under different UV irradiation conditions, for different industrial TiO_2 NPs concentrations on four different marine diatoms: *T. pseudonana, S. costatum, I. galbana, and D. teriolecta*. The test showed an inhibited growth under UV irradiation for all the algae except for *I. galbana*; the assumption made was that the main cause of inhibition is oxidative stress mediated by nano-TiO_2 high photo-activity, assumption which was later supported by measurements of increased oxygen radicals production as a function of nano-TiO_2 concentration.

UV irradiation was calibrated in order to reproduce oceanic surface conditions (UVA 4.5 W/m2 and UVB 4.1 W/m2). Each of the three affected diatom species showed a different no-effect concentration (NOEC) threshold, yet all of them showed growth inhibition after a certain concentration only under UV exposure; the measured thresholds are shown in Table 2.2, and the different responses of the diatoms to UV irradiation are shown in Figure 2.6, where it can be seen that without UV irradiation no toxic effects occurred on any of the tested diatoms.

Table 2.2. NOEC for four different diatoms exposed to TiO_2 nanoparticles.[21]

Diatom name	**NOEC [mg/l]**
I. galbana	<1
T. pseudonana	3
S. costatum	not detected
D. teriolecta	1-3

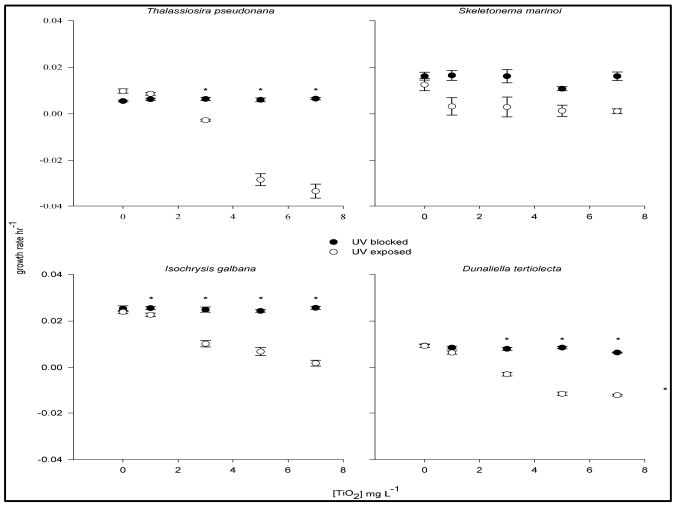

Figure 2.6. Effect of UV irradiation on TiO2 nanoparticles' toxicity towards four different diatoms.[21]

The study also highlighted the concern of ROS-induced stress on non-photosynthetic organisms. In fact, diatoms already live in hyperoxic conditions during photosynthesis, thus having naturally developed barriers against oxygen radicals. The same cannot be said for non-photosynthetic organisms, which therefore are into a potentially much greater danger.

Multiple studies on the release of metal ions from nano metal oxides as a potential toxicity mechanism toward different marine species were reviewed by Bondarenko O. et al.(2013)[22]. This toxicity mechanism is related mostly to particles with higher water solubility (such as ZnO and CuO), while it is less relevant for nearly insoluble particles such as TiO_2. To assess whether the toxicity is due to metal ions release, usually diverse metal salts are used (sulphates, chlorides, etc.), and the environmental responses to Metal Oxide NPs and metal salt are compared. Metal ion release-based toxicity is much more time dependent than nanoparticle toxicity, so an appropriate exposure time has to be elapsed during the analysis. In fact, after some time, nanoparticles tend to aggregate, strongly decreasing their toxic power, so dissolved metal ions remain the only toxic factor.

Metal oxide NPs have also shown mechanisms of cytotoxicity, by which the nanoparticles attach themselves to the organism, remain there even after washing and end up being adsorbed onto the cell membrane. However, other studies assume

that the toxicity does not have a direct relationship with surface adsorption of NPs, but with their electrostatic interaction with the membrane. Positively charged nanoparticles are attracted to the negatively charged bacteria, easing the adsorption on the outer membrane. It was found by Chang Y. (2012)[23] that a single nanoparticle is sufficient to disrupt a double layer lipid vesicle. Therefore, electrostatic interactions may have a significant role in NP toxicity.[23]

All of the cited experiments and the reviewed papers analyzed $nTiO_2$ toxicity with different methodologies, very few of which were standardized (OECD 201 guidelines[24] seem to be the most authoritative source of protocol). As a first step, a precise approach to $nTiO_2$ analysis should be developed according to said guidelines, to provide a milestone and a future consistent comparison for future toxicity studies and technological developments.

Then, it has been proved that commercial $nTiO_2$ is always different from nano-TiO_2 extracted by sunscreens or other PPCPs.[3] This often happens favoring a major complexity of $nTiO_2$ particles which are for example coated with other ENPs; since $nTiO_2$ is quite inert itself, a deep study of its interactions with coating agents and other toxics should be performed, in order to have a real estimate of the potential hazard posed by this new material. Finally, since phytoplankton species make the foundation of marine ecosystems, a little change in their amount, life cycle or chemical behavior could lead to unexpected consequences for the whole ecosystem.

Table 2.3. Review of toxicity studies performed on several nanoparticles and organisms

NP	Influencing factor(s)	Target species	Test method / conditions	Results	Thres-hold	Ref
TiO_2	Concentration, UV irradiation	*T. pseudonana, S. costatum, I. galbana, D. teriolecta*	20°C, 34 ppt salinity, 14:10 light:dark, 100–120 µmol/m^2s	non-toxic in unexposed cells, toxic under UV	3 mg/l n.d. <1 mg/l 1-3 mg/l	[21]
	pH, concentration, ionic strength,	*E. coli*	37°C, incubated in NP suspension (10-500 mg/l)	LC50 increasing with lower particle size. Rutile TiO2 almost non toxic	LC50 =17mg/l (variable NP size)	[25]
	concentration	*P. subcapitata*	24°C, 20ml+5ml f/2 medium	72 h LC 50	LC50=1,12mg/l	[26]
Ag	Particle size, concentration	*T. pseudonana*	16°C, ASW f/2, 13:11 light-dark, 100 rpm, pH 8.5	linear concentration-inhibition relation. 40um NP more effectve than 20um and 100 um	0.5 uM/20ml	[27]
	Particle size, concentration	*Synechococcus sp.*	26°C, Bg11, 12:12 light-dark, 120 rpm, pH 7.1	linear concentration-inhibition relation. 40nm NP more effectve than 20nm and 100 nm	3uM/20ml	[27]
	concentration	Algae (various)-crustaceans most sensitive specie	LC 50 data review	Very toxic [10]	LC50 =2,8 mg/l	[22]
CuO	concentration	Algae (various)-crustaceans most sensitive specie	LC 50 data review	Toxic [10]	LC50 =0,36 mg/l	[22]
	concentration	*P. subcapitata*	24°C, 20ml+5ml f/2 medium	72 h LC 50	LC50=0,43mg/l	[26]
ZnO	concentration	Algae (various)-also most sensitive specie	LC 50 data review	Very toxic [10]	LC50 =0,08 mg/l	[22]
	concentration	*P. subcapitata*	24°C, 20ml+5ml f/2 medium	72 h LC 50	LC50=0,01mg/l	[26]

Chapter 3 - Industrial nano-TiO_2 Toxicity Test

In this section, the experimental analysis that was performed in order to assess the toxicity of industrial TiO_2 nanoparticles towards the marine diatom *Thalassiosira pseudonana*, that was chosen as the target organism for this study, will be presented. The assessment of toxicity will be based on the percentage growth inhibition detected between specimens exposed to nano-TiO_2 and an uncontaminated sample, from now referred to as "control". All of the experiments were run at the Environmental Engineering Laboratory of the University of Miami.

The potential response of the marine environment to the variation of one or more factors is generally represented by a chosen model organism that has peculiar properties relevant to the study. Diatoms are often chosen as model organisms for marine toxicity studies given their relevance in the overall balance of the ecosystem: in fact, they account for the fixation of 40% of the total fixed carbon in the marine ecosystem[28], meaning that they provide a solid basement for the marine food chain, and due to their sensitivity to any physical or chemical variation in the environment.

The marine diatom *Thalassosira pseudonana* is often considered as a reliable model organism for both marine and freshwater environments, as a wide knowledge is available on it: its genome was completely sequenced[29], and its physical conformation has been widely investigated through a variety of techniques. Such level of knowledge makes it easier to track the impact of a variety of factors on the diatom, allowing to draw more general conclusions.

Reported mechanisms of toxicity of TiO_2 nanoparticles include genotoxicity[19,30] and surface adsorption[15], and *Thalassiosira pseudonana* has been already widely used to better understand the aforementioned mechanisms, thanks to the fact that its genome has been completely sequenced, and given the peculiar shape of its outer silica shell (cylindrical shape, with a complex pattern of nanopores)[31], which allows particular adsorption and internalization mechanisms. Moreover, the shell of *Thalassiosira pseudonana* is peculiar, as silica is a relatively refractory (melting point >1700 °C) and highly abrasive material, and such properties are already employed in industry. However, little or no knowledge is currently available on the

change in susceptibility to nanoparticle-mediated toxicity that silica shells imply when compared to the organic cell walls of other marine microalgae; therefore, further research effort needs to be devoted to the clarification of the role of silica shells in the observed macroscopic toxic effects.

Given that the purpose of this study is to investigate the toxic effects of different types of TiO_2 nanoparticles suspended in artificial seawater, and given the variety of toxicity mechanisms that have already been reported for these nanoparticles, the chosen target organism for this study was the marine diatom *Thalassiosira pseudonana*, being it one of the most significant organisms in the marine environment, given its sensitivity to environmental modifications and fundamental role in the food chain and chemical balance of the ecosystem.

3.1 Technical equipment

After having received proper training from experienced personnel, Ph. D. students, and from online courses (completed the required modules from the Collaborative Institutional Training Initiative -C.I.T.I.- Program), the following equipment was used for the purposes of this study and will be now introduced.

3.1.1 Beckman Coulter DU 720 - Spectrophotometer

In order to determine the differences in diatom growth, it was decided to use the light absorbance of the tested samples. In order to do so, a DU 720 UV/Vis Spectrophotometer[32] (Beckman Coulter, DU® 720, Pasadena, CA) was used; it can be observed in Figure 3.1. The spectrophotometer that was used can detect wavelengths in the range of 190-1100 nm, and measure the light absorbance with an accuracy of 0.001 Abs. The operational protocol of the spectrophotometer requires to:

- Define the wavelength range to be tested,
- Scan a “blank” specimen (ultrapure water) in order to calibrate the device, and
- Scan all the tested samples. (use a 3mL specimen)

Figure 3.1. DU 720 UV/Vis Spectrophotometer.[32]

3.1.2 Nano ZS90 – Zeta-sizer

The device that was used in order to carry over the measurements of particle size and zeta potential that were necessary to further characterize the colloidal suspensions formed by the tested nanoparticles was the Nano ZS90 Zeta-sizer[33] (Malvern Instruments, UK) that is shown in Figure 3.2. Particle sizes (diameter) that can be measured range from 0.3 nm to 5.0 µm. Zeta potential can be measured for particles ranging from 3.8 nm to 100 µm (diameter), with an accuracy of 0.12 µm cm/Vs. The operational protocol for the Nano ZS90 Zeta-sizer requires to:

- Wash the cuvettes with ethanol,
- Fill the size-measurement cuvette up to the appropriate mark,
- Insert the cuvette in the zeta-sizer and run the measurement,
- Remove the size-measurement cuvette,

- Fill the zeta potential-measurement cuvette appropriately, and
- Insert the cuvette in the zeta-sizer and run the measurement.

Figure 3.2. Nano ZS90 zeta-sizer[33] (Malvern Instruments, UK), and the special cuvettes used to measure zeta potential (left) and particle size (right).

3.1.3 Verilux VT 10 - 5000 lux white UV Lamp

The culture conditions of the test samples were defined in accordance with existing literature, and the samples were stored in an incubator at a constant temperature T=26°C, being subjected to 12h dark:light cycles of white UV light, in order to recreate the ideal growth conditions for the marine diatom *Thalassiosira pseudonana.* The illumination was provided by the Verilux VT 10 - 5000 lux[34] (Verilux, VT) lamp, shown in Figure 3.3, which was regulated by means of a timer that switched it every 12 hours.

Figure 3.3. Verilux VT 10 Lamp - 5000 lux[34] (Verilux, VY), white UV light, shown in the incubator together with a Petri dish and two cell Mass Cultures.

3.1.4 Orion™ pH-meter

The pH of the solution needs to be measured at the beginning and at the end of the experiment, as well as whenever zeta potential and particle size measurements are performed, in order to be able to plot the IEP (Isoelectric Point) of the measured nanoparticles and to keep track of possible changes in the sample. The monitoring of ph was achieved using the Orion™ 720Aplus pH-meter [35](Thermo Fisher Scientific, MA) (Figure 34), in combination with the glass electrode Orion™ 8156BNUWP[35] (Thermo Fisher Scientific, MA).

Figure 3.4. Orion™ 720Aplus pH-meter[35] and glass electrode on its support.

3.2 Manufacture of artificial seawater and f/2 medium

In order to recreate the natural marine environment in which the tested diatom Thalassiosira pseudonana lives and reproduces, while maintaining standardized experimental conditions, Artificial Sea Water (ASW) and f/2 medium were used in each diatom culture. Guillard's f/2 medium is among the recommended live foods for aquaculture from FAO[36] for its composition and nutrients, along with Walne's medium (equivalent, not used in this study). Artificial Seawater and f/2 medium were prepared in the laboratory according to Guillard et al. (1962)[37] and Keller et al. (1988)[38].

3.2.1 Preparation of artificial sea water

For the preparation of Artificial Sea Water, the salts shown in Table 3.1 have to be dissolved in 1 liter of ultrapure water (18.2 MΩ) produced with a three-stage Millipore Milli-Q plus 185 purification system (Millipore, Billerica, MA):

Table 3.1. Salts to be dissolved in Ultrapure water to obtain Artificial Sea Water

Salt	Weight (g)	Purity	Vendor	City, State
NaCl	27.72	>99.0%	Fischer Scientific	Fair Lawn, NJ
KCl	0.67	99.7%	Sigma-Aldrich	St. Louis, MO
$CaCl_2$	1.03	>99.0%	Sigma-Aldrich	St. Louis, MO
$MgCl_2$	4.66	>99.0%	BDH Chemicals	Radnor, PA
$MgSO_4$	3.07	>99.5%	Sigma-Aldrich	St. Louis, MO
$NaHCO_3$	0.18	99.9%	Mallinckrodt	Paris, KY

Once prepared, Artificial Sea Water is adjusted to a pH=8.0 by the progressive addition of 1 M NaOH or HCl; the pH was monitored with the pH-measurement apparatus that has been illustrated in Section 3.1.4.

3.2.2 Preparation of f/2 medium

The f/2 medium is a common addition to Artificial Sea Water in order to provide the ideal amount of chemicals and nutrients necessary to marine and coastal diatoms to thrive and reproduce. The name "f/2 medium" comes from the fact that the concentration given in the original formulation of this medium, named "f medium" (Guillard et al., 1962)[37], has been reduced by a factor 2. The composition of f/2 medium is listed in Table 3.2; the prescribed quantities are to be added to an initial volume of 950 ml of ASW, which has then to be adjusted to a final volume of 1 l.

Table 3.2. f/2 medium composition.[37]

Component	Stock solution	Quantity (ml)	Concentration
$NaNo_3$	75 g/L	1	8.82×10^{-4} M
NaH_2PO_4H2O	5 g/L	1	3.62×10^{-5} M
Trace metal solution	-	1	-
Vitamin solution	-	0.5	-

The detailed compositions of the trace metal solution and of the vitamin solution are shown in tables 3.3 and 3.4, respectively. The indicated stock solutions required for the making of the Trace Metal solution have to be prepared separately. The amounts indicated in the column "Quantity" are to be added to an initial volume of 950 ml ASW, which will be then adjusted to a final volume of 1l by the addition of ASW.

Table 3.3. Trace Metal solution composition.[37]

Component	**Stock solution**	**Quantity**	**Concentration**
$FeCl_3$ 6H2O	-	3.15 g	1.17×10^{-5} M
Na_2 EDTA 2H2O	-	4.36 g	1.17×10^{-5} M
$CuSO_4$ $5H_2O$	9.8 g/L H_2O	1 mL	3.93×10^{-8} M
Na_2MoO_4 $2H_2O$	6.3 g/L H_2O	1 mL	2.60×10^{-8} M
$ZnSO_4$ $7H_2O$	22.0 g/L H_2O	1 mL	7.65×10^{-8} M
$CoCl_2$ $6H_2O$	10.0 g/L H_2O	1 mL	4.20×10^{-8} M
$MnCl_2$ $4H_2O$	180.0 g/L H_2O	1 mL	9.10×10^{-7} M

The necessary components for the preparation of the Vitamin solution are presented in Table 3.4; the listed quantities are added to an initial volume 950 mL of ASW, and then adjusted to a final volume of 1 l by the addition of ASW.

Table 3.4. Vitamin solution composition.[37]

Component	**Stock solution**	**Quantity**	**Concentration**
Thiamine HCl (vit. B1)	-	200 mg	2.96×10^{-7} M

Biotin (vit. H)	1.0 g/L H_2O	1 mL	2.05 x 10^{-9} M
Cyanocobalamin (vit B12)	1.0 g/L H_2O	1 mL	3.69 x 10^{-10} M

3.3 Nanoparticles

Commercial TiO_2 nanopowder (>99.7% purity, <25nm particle size, 45–55 m^2/g surface area, anatase) was purchased from Sigma-Aldrich[39] (St. Louis, MO). The set of tested effective concentrations for industrial TiO_2 nanoparticles was 1.0 mg/l, 2.5 mg/l, and 5.0 mg/l, obtained by adding the required amount of nanopowder to the final volume of diatom culture and ASW + f/2 medium.

3.4 Diatom culture

Thalassiosira pseudonana cells were purchased from Bigelow Laboratory for Ocean Sciences (CCMP 1335)[40]. The culture was created by adding the purchased cells to a 1L mass flask containing ASW + f/2 medium. The culture was then incubated at a constant temperature of 26°C, with 12h:12h (dark:light) cycles using the Verilux VT 10 white UV lamp illustrated in Section 3.1.3.

3.5 Experimental setup

In order to perform the designed growth inhibition tests, both the diatom culture and the TiO_2 nanoparticles needed to be characterized in terms of absorbance, defining the peak absorbance wavelength for each of them. In fact, if the peak absorbance wavelengths of diatoms and nanoparticles were too close one to the other (i.e., enough to cause overlapping of absorbance peaks), the absorbance measurement would not have been a reliable indicator, and alternative ways to assess toxicity would have had to be found.

3.5.1 Detection of *T. pseudonana* peak absorbance wavelength

In the present study, several measurements of absorbance were performed on control samples and on samples that were exposed to TiO_2 nanoparticles under designated conditions. Absorbance was chosen as an indirect measurement of growth inhibition: the rationale behind this choice was that, under the condition that

nanoparticles and diatoms had different and non-overlapping absorbance peaks, a lower absorbance in a contaminated sample would represent a decrease in diatom growth (i.e., growth inhibition), which has to be ascribed to the exposure to TiO_2 nanoparticles, since they are the only modification made with respect to the control sample.

Prior to proceeding to the growth inhibition tests, the peak absorbance wavelength of the chosen target organism, *Thalassiosira pseudonana*, needed to be assessed. Given the wide range of wavelengths that the spectrophotometer can scan (i.e. 190-1100 nm, see Section 3.1.1), the range was preliminarily narrowed down by conducting a literature search on peak absorbance wavelengths for *Thalassiosira pseudonana* that were recorded in previous studies.

A study from Sobrino et al. (2008)[41] recorded the specific absorbance of the diatom *Thalassiosira pseudonana*, ranging from 290 nm to 750 nm. In this study, a clear absorbance peak was found between 650 nm and 690 nm, as it can be seen in Figure 3.5.

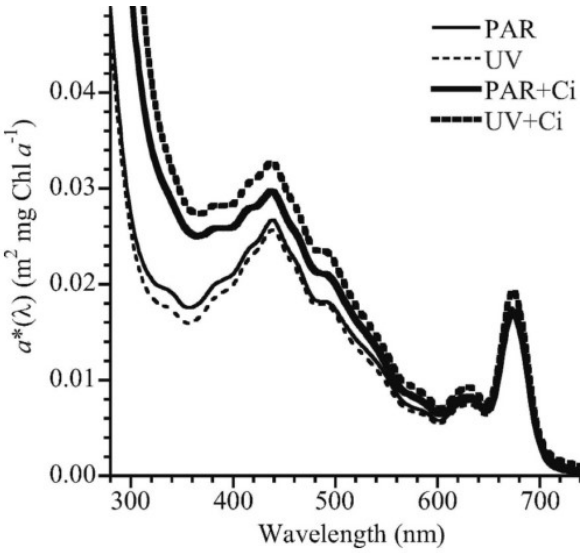

Figure 3.5. Absorbance spectrum of marine diatom *Thalassiosira pseudonana* under different culture conditions.[41]

The second study that was considered to assess the peak absorbance wavelength was a work from Davis et al. (2006)[42]: in this study, the culture of *Thalassiosira*

pseudonana was purchased by our same vendor (Bigelow Laboratory for Ocean Sciences, see Section 3.4), therefore it seemed reasonable to give credit to the emission wavelength that was used to monitor algal growth. In this case, the monitored wavelength has been near 670 nm.

Based on the reported works, we narrowed the inspected range of wavelength, starting from a 600 to 700 nm range, and moving the extremes that had lower absorbance. Once we reached a satisfying precision, having reduced the range of peak absorbance wavelengths to 668 to 679 nm, we further refined this range.

In order to do so, we measured and recorded the absorbance values of the cell culture (marine diatoms and ASW + f/2 medium, see Section 3.4), over the entire range (668-679 nm), performing the measurements at serial dilutions, with a dilution factor equal to 2 (i.e., after each measurement, the cell culture was diluted with ultrapure water to half of its original concentration).

A total of 8 dilutions were performed, reaching 1:256 of the initial concentration; at such dilution, the detection limit of the spectrophotometer was encountered (i.e. the measured absorbance was equal to 0.001, see Section 3.1.1), and therefore further dilutions would have been undetectable.

Absorbance values at each dilution were measured over the selected range and recorded, as it can be seen in Table 3.5. The performed measurement highlighted a peak absorbance wavelength of λ=674 nm, which was then assumed as the peak absorbance wavelength for the diatom *Thalassiosira pseudonana*, for all the purposes of this study.

Table 3.5. Light absorbance values of *Thalassiosira pseudonana* measured at different wavelengths and serial dilutions.

		Wavelength (nm)						
		670	672	673	674	675	677	679
Dilution Factor	1	0.146	0.15	0.15	0.151	0.15	0.148	0.145
	2	0.077	0.079	0.079	0.079	0.079	0.078	0.076
	4	0.038	0.039	0.039	0.040	0.039	0.039	0.038
	8	0.020	0.020	0.020	0.020	0.020	0.020	0.020
	16	0.012	0.013	0.013	0.013	0.013	0.013	0.012
	32	0.005	0.005	0.005	0.005	0.005	0.005	0.005
	64	0.003	0.003	0.003	0.003	0.003	0.003	0.003
	128	0.001	0.002	0.002	0.002	0.002	0.001	0.001
	256	0.001	0.001	0.001	0.001	0.001	0.001	0.001

The absorbance values for λ=674 nm at each dilution were plotted on a Cartesian plan, and a trend line was calculated for the obtained (dilution, absorbance) set of points, to further assess the reliability of the chosen wavelength.

As a result, a linear relationship between absorbance and dilution factor was found, in agreement with our expectations (a decrease in the cell amount should lead to the same decrease in absorbance). The plot of the regression line is shown in Figure 3.6.

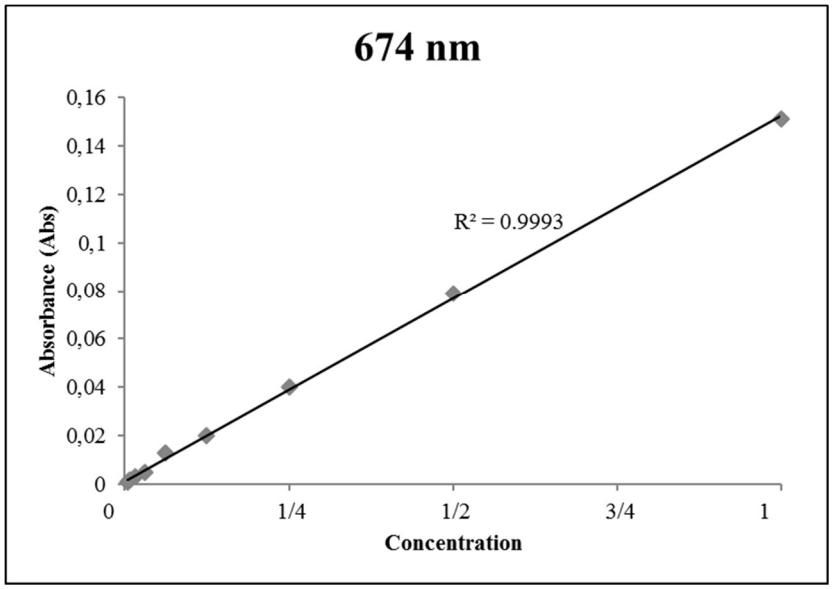

Figure 3.6. Regression line for the peak absorbance wavelength of *Thalassiosira pseudonana*, λ=674 nm.

R^2=0.9993 further confirmed the reliability of the calibration experiment and allowed us to move onto the following steps of the experiments.

3.5.2 Detection of nano-TiO_2 peak absorbance wavelength

As it was anticipated, the indirect estimation of growth inhibition (i.e., TiO_2 nanoparticles' toxicity) by mean of absorbance measurements could only considered reliable in the case that the two peaks of light absorbance given by the diatom *Thalassiosira pseudonana* and by TiO_2 nanoparticles occurred at significantly different wavelengths, in order to avoid any kind of interference and subsequent misinterpretation. Therefore, the peak absorbance wavelength of TiO_2 nanoparticles had to be determined.

The procedure used was similar to the one illustrated in the previous section and used to determine the peak absorption wavelength of *Thalassiosira pseudonana:* absorbance measurements are performed on a colloidal suspension of TiO_2 in ASW + f/2 medium, on a reasonably restricted range of wavelengths, and progressively diluting the original sample; the tested set of concentration was [100; 50; 20; 10; 5; 2; 1; 0.5; 0.25; 0,13] mg/L. In this way, we wanted to test the spectrophotometer for an upper and for a lower bound in detection limits, by measuring the absorbance of a

highly concentrated solution and by diluting the tested sample until the Limit of Detection (LOD).

Reported values in existing literature for TiO_2 peak absorbance wavelength vary in the range of 250 – 450 nm[43,44], as it can be seen in Figure 3.7 and Figure 3.8; therefore, the initial range was narrowed down qualitatively, using the absorbance plot function provided by the spectrophotometer. This allowed to assess a peak absorbance wavelength equal to λ=350 nm for the colloidal suspension of TiO_2 in ASW + f/2 medium.

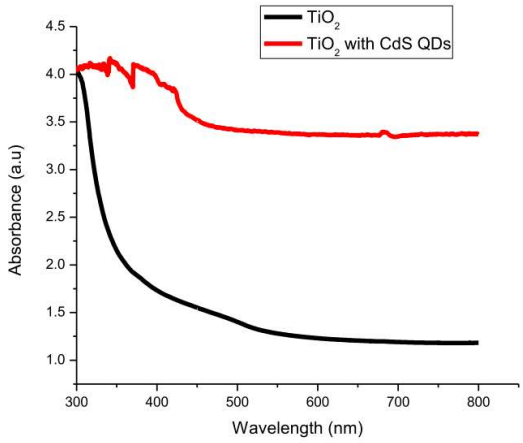

Figure 3.7. Absorbance spectrum of visible light of Titanium Dioxide in different conditions.[43]

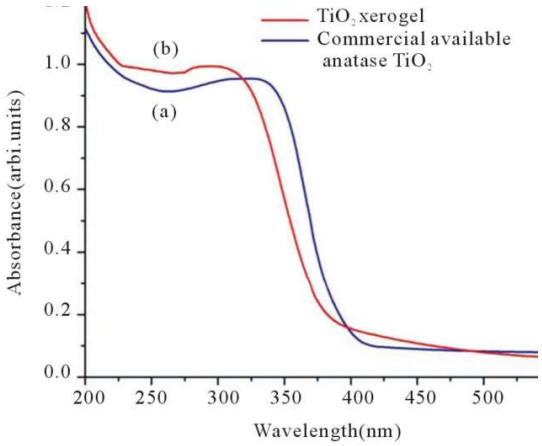

Figure 3.8. Absorbance spectrum of Titanium Dioxide in different forms.[44]

The results of the absorbance calibration test were plotted on a Cartesian plan, and a trend line was calculated for the obtained (concentration, absorbance) set of points, to further assess the reliability of the chosen wavelength.

As a result, a linear relationship between absorbance and dilution factor was found, in agreement with our expectations and with the findings that have been reported in the previous section. The R^2=0.9957 further confirmed the reliability of the results. The results are shown in Table 3.6 and in Figure 3.9.

Table 3.6. Results of the absorbance calibration test for industrial TiO2 nanoparticles; Detection Limit: 0.13 mg/L.

TiO_2 conc. (mg/L)	**Abs**
LOD - 0.13	0.001
0.25	0.002
0.5	0.003
1	0.004
2	0.007
5	0.014
10	0.028
20	0.036
50	0.114
100	0.244

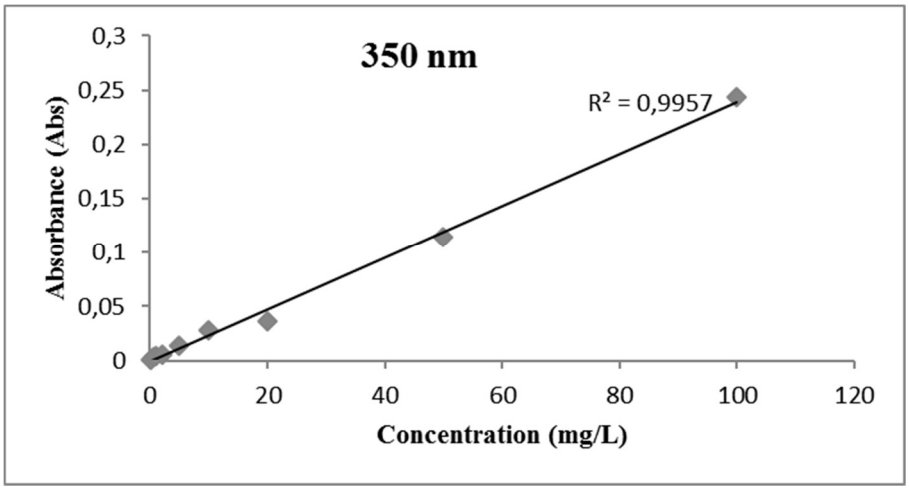

Figure 3.9. Regression line for the peak absorbance wavelength of industrial TiO_2 nanoparticles, λ=350 nm.

3.5.3 Growth inhibition (%) as a function of exposure time

In this set of experiments, all of the tests were performed in triplicate copy. Each test sample was made by adding 15 mL of colloidal suspension of TiO_2 in ASW + f/2 medium to 15 mL of diatom culture (see Section 3.4 for reference) into a 50 mL Petri dish. The control samples (also triplicate) were prepared by adding 15 mL of ASW + f/2 medium to 15 mL of diatom culture into a 50 mL Petri dish. After having gently mixed each sample, they were tested for absorbance (see section 3.1.1 for operational protocol). After the absorbance measurement, the samples were put in the incubator, under the conditions stated in Section 3.1.4.

Absorbance measurements were repeated at scheduled times: 5h, 12h, 24h, 48h, 72h, and 96h.

The concentrations of industrial TiO_2 nanoparticles that were tested in this experiment were 2.5 mg/L and 5.0 mg/L.

The pH was measured at the beginning and at the end of the experiment using the pH-meter illustrated in section 3.1.4.

3.5.4 Growth inhibition (%) as a function of concentration

In this set of experiments, all of the tests were performed in triplicate copy. Each test sample was made by adding 15 mL of colloidal suspension of TiO_2 in ASW + f/2 medium to 15 mL of diatom culture (see Section 3.4 for reference) into a 50 mL Petri dish. The control samples (also triplicate) were prepared by adding 15 mL of ASW + f/2 medium to 15 mL of diatom culture into a 50 mL Petri dish. After having gently mixed each sample, they were tested for absorbance (see section 3.1.1 for operational protocol). After the absorbance measurement, the samples were put in the incubator, under the conditions stated in Section 3.1.4.

The samples were tested again for absorbance after a fixed elapsed time, t=72h.

The concentrations of industrial TiO_2 nanoparticles that were tested in this experiment were 1.0 mg/L, 2.5 mg/L, and 5.0 mg/L.

The pH was measured at the beginning and at the end of the experiment using the pH-meter illustrated in section 3.1.4.

3.5.5 Monitoring of particle size, zeta potential, and pH

Hydrodynamic particle size and zeta potential were measured at the beginning of the experiment and at time steps of 5h, 12h, 24h, 48h and 72h (the latter was previously assessed to be the break-through time), by using the Nano ZS90 zetasizer illustrated in Section 3.1.2, following the measurement protocol illustrated in the same section.

pH was measured at the beginning of the experiment and at time steps of 5h, 12h, 24h, 48h and 72h (the latter was previously assessed to be the break-through time), by using the OrionTM pH-meter illustrated in Section 3.1.4. The measurements were performed by immersing the glass electrode in the sample, and then waiting for the stabilization before performing the reading of the current pH value.

All of the aforementioned measurements have been performed both on the control sample (see Section 3.5.3 for composition and preparation) and on the diatom cultures exposed to a 5 mg/L concentration of TiO_2 nanoparticles.

3.6 Results

3.6.1 Particle size, zeta potential, and pH

The measurements for all of the cultures exposed to 5 mg/L colloidal suspensions of industrial, toothpaste-derived, and sunscreen-derived TiO2 nanoparticles are synthesized in Figure 5.3.

For industrial TiO2 nanoparticles, it can be seen that particle size experienced a net increase during the exposure time, going from an initial size of 70 nm to a final size of 81 nm. However, the particle size changed following a non-linear pattern, increasing until t=24h to a peak of 181nm, and then decreasing sharply.

The surface charge was relatively low immediately after injecting the colloidal suspension, at a value of -4.75 mV. After 5h, however, it increased its absolute value significantly up to -7.73 mV; from that time, it decreased its absolute value, reaching -5.72 mV.

The measured value of pH decreased slightly and rather linearly during time, going from 8.47 to 7.24.

3.6.2 Growth inhibition (%) as a function of exposure time

The measured values of absorbance and the calculated values of growth inhibition will be shown in the following page. At each time, triplicate values of absorbance were recorded both for the control sample and for every other test sample. A statistical analysis was conducted on each triplicate experiment, computing statistically relevant parameters such as average, variance, standard error on mean (i.e., SEM), and performing the student *t*-test, in order to assess its statistical significance.

The average values were then used to compute growth inhibition, according to the correlation proposed by Cao et al. (2011)[45]:

$$GI\ (Growth\ Inhibition, \%) = \frac{\overline{abs_{control}} - \overline{abs_{sample}}}{\overline{abs_{control}}} \cdot 100$$

The absorbance values used in the calculation are the average for each triplicate set.

The statistical parameters that were computed for this set of experiments are, as anticipated:

- Standard deviation: this parameter allows to determine how disperse each triplicate set was. $\bar{x}$ represents the average for the triplicate set.

$$\sigma = \sqrt{\frac{\sum(x-\bar{x})^2}{(n-1)}}$$

- Standard error on mean (i.e., SEM): SEM is a measure of the precision of the mean.

$$SEM = \frac{\sigma}{\sqrt{n}}$$

- The student *t*-test was performed for all of the triplicate experiments, in order to assess their statistical significance. The test was conducted under the assumption of having two samples with equal variance. All of the tested concentrations showed statistical significance after t=96h (having $p<0.05$).

Following are the tables and plots summarizing the data, statistical analysis and results of the time-dependent toxicity test at the concentrations of 2.5 mg/L and 5.0 mg/L.

Table 3.7. Dataset and results for inhibition as a function of exposure time; industrial nano-TiO_2, 2.5 mg/L

concentration	2,5 mg/L						
time	0	5	12	24	48	72	96
control 1	0,020	0,023	0,021	0,027	0,044	0,083	0,104
control 2	0,022	0,023	0,020	0,024	0,044	0,080	0,098
control 3	0,023	0,020	0,019	0,023	0,045	0,079	0,104
AVG	0,022	0,022	0,020	0,025	0,044	0,081	0,102
ST DEV	0,002	0,002	0,001	0,002	0,001	0,002	0,003
SEM	0,001	0,001	0,001	0,001	0,000	0,001	0,002
Indust. TiO2 1	0,026	0,021	0,019	0,024	0,038	0,044	0,065
Indust. TiO2 2	0,027	0,026	0,023	0,026	0,037	0,048	0,069
Indust. TiO2 3	0,027	0,024	0,022	0,023	0,038	0,046	0,071
AVG	0,027	0,024	0,021	0,024	0,038	0,046	0,068
ST DEV	0,001	0,003	0,002	0,002	0,001	0,002	0,003
SEM	0,000	0,001	0,001	0,001	0,000	0,001	0,002
G.I. (%)	\	-8,12	-7,09	0,93	15,03	42,92	32,94
G.I. (%) ST DEV	\	7,48	7,20	4,88	0,61	1,82	2,05
G.I. (%) SEM	\	4,32	4,15	2,82	0,35	1,05	1,18

Table 3.8. Dataset and results for inhibition as a function of exposure time; industrial nano-TiO_2, 5.0 mg/L

concentration	5 mg/L						
time (h)	0	5	12	24	48	72	96
control 1	0,029	0,024	0,020	0,032	0,043	0,100	0,119
control 2	0,027	0,024	0,022	0,031	0,048	0,103	0,122
control 3	0,027	0,026	0,020	0,033	0,047	0,106	0,126
AVG	0,028	0,025	0,021	0,032	0,046	0,103	0,122
ST DEV	0,001	0,001	0,001	0,001	0,003	0,003	0,004
SEM	0,001	0,001	0,001	0,001	0,002	0,002	0,002
TiO2 1	0,034	0,024	0,020	0,031	0,047	0,085	0,085
TiO2 2	0,031	0,024	0,020	0,031	0,046	0,091	0,091
TiO2 3	0,030	0,025	0,021	0,031	0,044	0,102	0,102
AVG	0,032	0,024	0,020	0,031	0,046	0,093	0,093
ST DEV	0,002	0,001	0,001	0,000	0,002	0,009	0,009
SEM	0,001	0,000	0,000	0,000	0,001	0,005	0,005
G.I. (%)	\	1,28	1,36	3,06	0,42	10,14	24,34
G.I. (%) ST DEV	\	1,11	3,57	1,52	4,24	2,88	2,43
G.I. (%) SEM	\	0,64	2,06	0,87	2,45	1,66	1,40

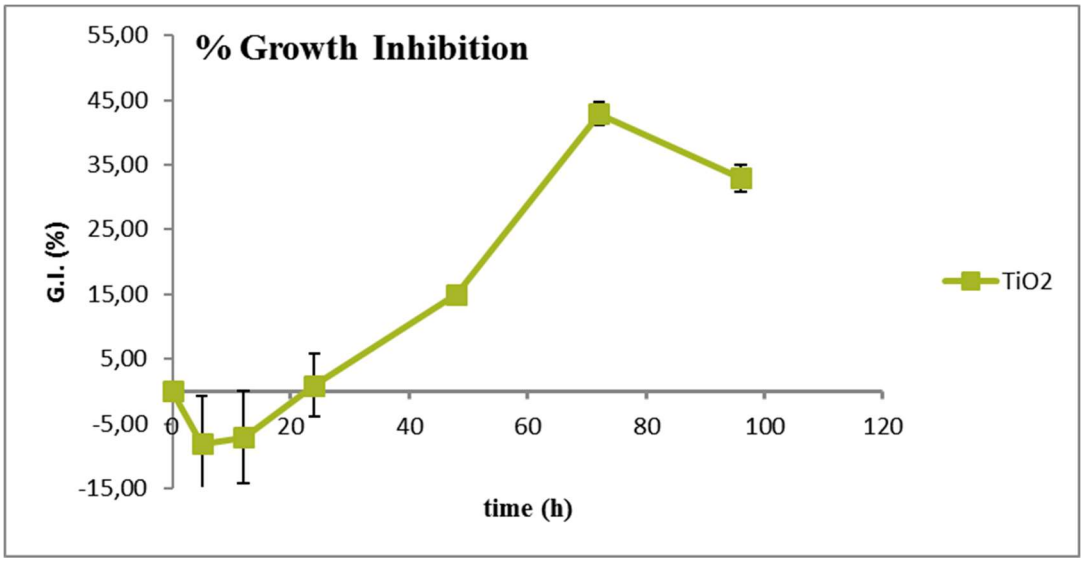

Figure 3.10. % Growth inhibition of *Thalassiosira pseudonana* as a function of exposure time; industrial nano-TiO_2, 2.5 mg/L

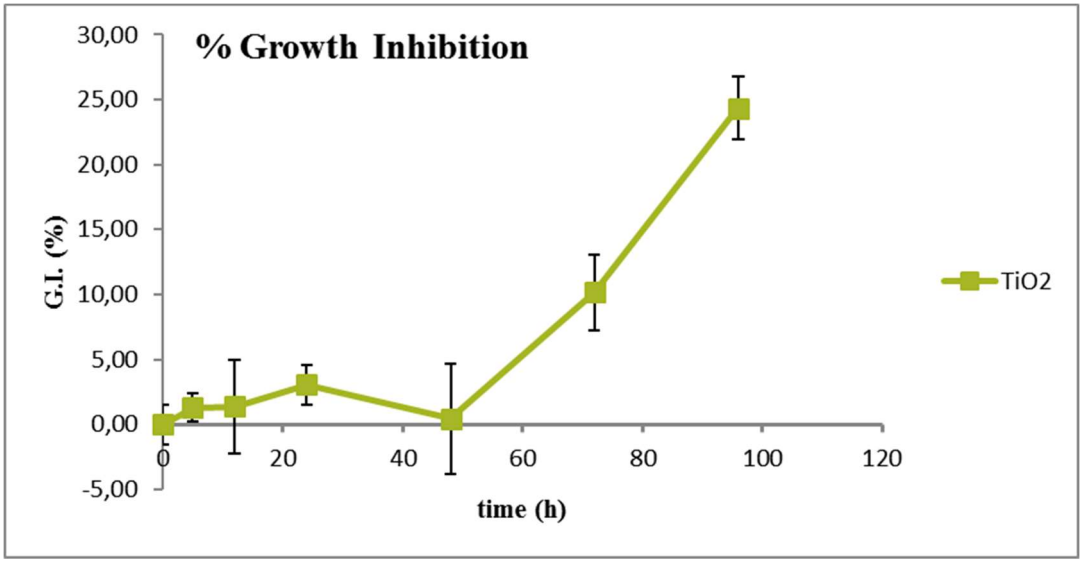

Figure 3.11. % Growth inhibition of *Thalassiosira pseudonana* as a function of exposure time; industrial nano-TiO_2, 5.0 mg/L

The task of the present set of experiments was to assess whether exposure time had a significant impact on the toxicity exerted by industrial nano-TiO_2 towards Thalassiosira pseudonana.

As it can be observed from both Figure 3.10 and Figure 3.11, a significant increase in % growth inhibition occurs after t=72h, while the preceeding growth inhibition is almost negligible and/or flawed by high standard deviations.

This can be explained analyzing the typical cellular growth curve, shown in Figure 3.12: cellular growth is initially characterized by a lag-phase, during which almost no growth can be observed on the population. After the lag-phase, a sudden increase in the slope of the plot (i.e. growth rate, growth per unit time) can be observed: this is the so-called log-phase, during which an evident increase (logaritmic growth rate) of the cell population can be observed. After this phase, a stationary phase (no growth) and a decline phase (negative growth rate) are present.

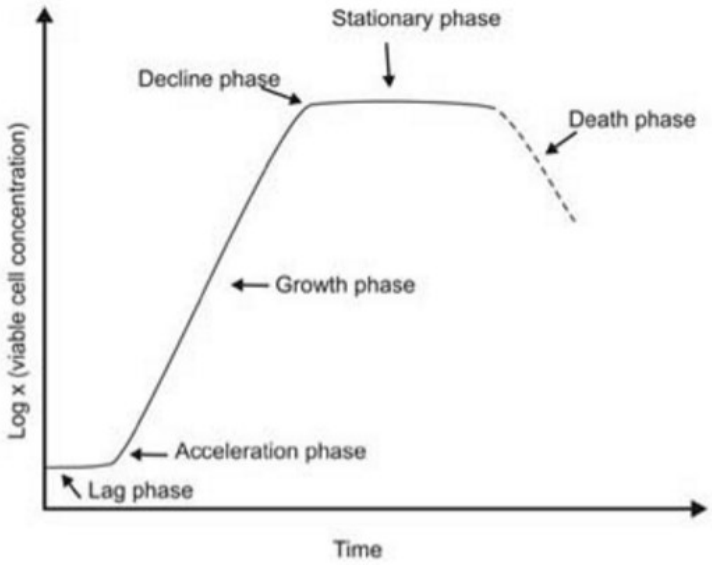

Figure 3.12. Typical cell growth curve.[46]

The initially low growth inhibition is due to the fact that no diatom growth is likely to occur at all during the first phase, thus reducing the potential for growth inhibition.

Our plots have a strong resemblance with the first two phases of the cellular growth curve, that can be therefore used to justify the existence of a break-through time between 48h and 72h from inoculation (i.e. acceleration phase). Given the

intrinsic variability involved in cell growth, it was concluded that t=72h was the proper breakthrough time for the tested system.

3.6.3 Growth inhibition (%) as a function of concentration

The measured values of absorbance and the calculated values of growth inhibition will be shown in the following page. At t=0h and t=72h (previously assessed as a proper break-through time), triplicate values of absorbance were recorded both for the control sample and for every other test sample. A statistical analysis was conducted on each triplicate experiment, computing statistically relevant parameters such as average, variance, standard error on mean (i.e., SEM), and performing the student *t*-test, in order to assess its statistical significance.

The average values were then used to compute growth inhibition, according to the correlation proposed by Cao et al. (2011)[45]:

$$GI\ (Growth\ Inhibition, \%) = \frac{\overline{abs_{control}} - \overline{abs_{sample}}}{\overline{abs_{control}}} \cdot 100$$

The absorbance values used in the calculation are the average for each triplicate set.

The statistical parameters that were computed for this set of experiments are, as anticipated:

- Standard deviation: this parameter allows to determine how disperse each triplicate set was. $\bar{x}$ represents the average for the triplicate set.

$$\sigma = \sqrt{\frac{\sum(x-\bar{x})^2}{(n-1)}}$$

- Standard error on mean (i.e., SEM): SEM is a measure of the precision of the mean.

$$SEM = \frac{\sigma}{\sqrt{n}}$$

- The Pearson Correlation Coefficient was computed for concentration versus percent growth inhibition.

$$r = \frac{\sum[(conc - \overline{conc})(G.I. - \overline{G.I.})]}{\sqrt{\sum[(conc - \overline{conc})^2 (G.I. - \overline{G.I.})^2]}}$$

The computed correlation coefficient between concentration and percent growth inhibition for industrial TiO_2 nanoparticles is equal to 0,991, thus showing high positive correlation between the aforementioned parameters.

Following are the tables and plots summarizing the data, statistical analysis and results of the concentration-dependent toxicity test at the concentrations of 1.0 mg/L, 2.5 mg/L, and 5.0 mg/L.

Table 3.9. Dataset and results for inhibition as a function of concentration at breakthrough time t=72h.

Sample	abs (t=0h)	abs (t=72h)	G.I. (%)	G.I. (%) ST. DEV	G.I. (%) SEM
Control 1	0,010	0,030			
Control 2	0,010	0,028	/	/	/
Control 3	0,009	0,023			
IND TiO2 1mg/l #1	0,01300	0,02700			
IND TiO2 1mg/l #2	0,01300	0,02500	3,70370	2,70000	1,55885
IND TiO2 1mg/l #3	0,01300	0,02600			
IND TiO2 2.5mg/l #1	0,01100	0,02600			
IND TiO2 2.5mg/l #2	0,012	0,024	6,17284	1,87061	1,08000
IND TiO2 2.5mg/l #3	0,010	0,026			
IND TiO2 5mg/l #1	0,015	0,023			
IND TiO2 5mg/l #2	0,010	0,024	13,58025	0,42514	0,24545
IND TiO2 5mg/l #3	0,013	0,023			

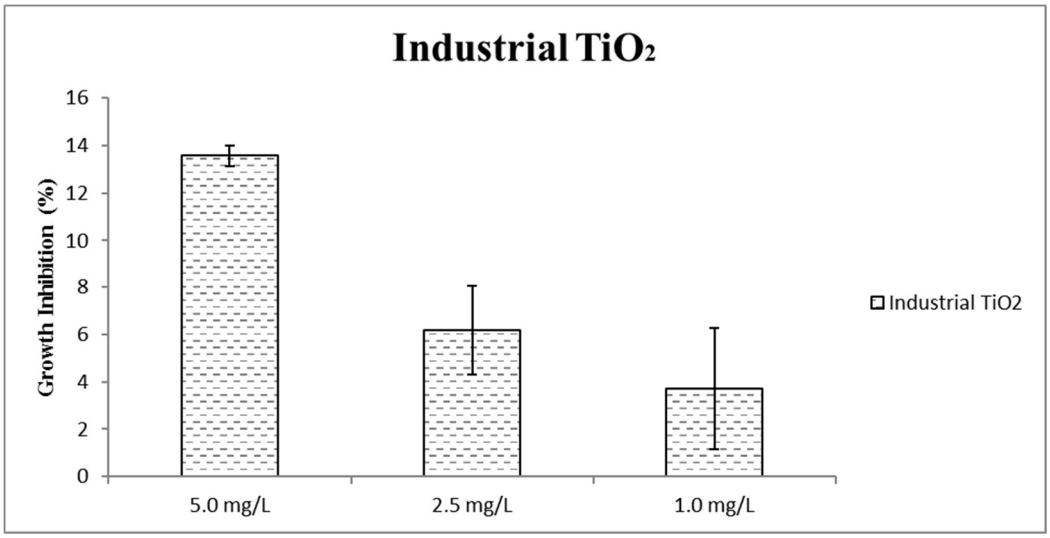

Figure 3.13. % Growth inhibition of *Thalassiosira pseudonana* as a function of concentration; measured at breakthrough time t=72h.

Chapter 4 – Product-derived nano-TiO2 Toxicity

In this section, the experimental analysis that was performed in order to assess the toxicity of sunscreen-derived and toothpaste-derived TiO_2 nanoparticles towards the marine diatom *Thalassiosira pseudonana*, that was chosen as the target organism for this study, will be presented. The assessment of toxicity will be based on the percentage growth inhibition detected between specimens exposed to nano-TiO_2 and the control sample. All of the experiments were run at the Environmental Engineering Laboratory of the University of Miami.

4.1 Technical equipment

The following equipment was used for the purposes of this study and will be now introduced.

4.1.1 Beckman Coulter DU 720 - Spectrophotometer

In order to determine the differences in diatom growth, it was decided to use the light absorbance of the tested samples. In order to do so, a DU 720 UV/Vis Spectrophotometer[32] (Beckman Coulter, DU® 720, Pasadena, CA) was used; it can be observed in Figure 3.1. The spectrophotometer that was used can detect wavelengths in the range of 190-1100 nm, and measure the light absorbance with an accuracy of 0.001 Abs. The operational protocol of the spectrophotometer requires to:

- Define the wavelength range to be tested,
- Scan a "blank" specimen (ultrapure water) in order to calibrate the device, and
- Scan all the tested samples. (use a 3mL specimen)

4.1.2 Nano ZS90 – Zeta-sizer

The device that was used in order to carry over the measurements of particle size and zeta potential that were necessary to further characterize the colloidal

suspensions formed by the tested nanoparticles was the Nano ZS90 Zeta-sizer[33] (Malvern Instruments, UK) that is shown in Figure 3.2. Particle sizes (diameter) that can be measured range from 0.3 nm to 5.0 μm. Zeta potential can be measured for particles ranging from 3.8 nm to 100 μm (diameter), with an accuracy of 0.12 μm cm/Vs. The operational protocol for the Nano ZS90 Zeta-sizer requires to:

- Wash the cuvettes with ethanol,
- Fill the size-measurement cuvette up to the appropriate mark,
- Insert the cuvette in the zeta-sizer and run the measurement,
- Remove the size-measurement cuvette,
- Fill the zeta potential-measurement cuvette appropriately, and
- Insert the cuvette in the zeta-sizer and run the measurement.

4.1.3 Verilux VT 10 - 5000 lux white UV Lamp

The culture conditions of the test samples were defined in accordance with existing literature, and the samples were stored in an incubator at a constant temperature T=26°C, being subjected to 12h dark:light cycles of white UV light, in order to recreate the ideal growth conditions for the marine diatom *Thalassiosira pseudonana.* The illumination was provided by the Verilux VT 10 - 5000 lux[34] (Verilux, VT) lamp, shown in Figure 3.3, which was regulated by means of a timer that switched it every 12 hours.

4.1.4 Orion™ pH-meter

The pH of the solution needs to be measured at the beginning and at the end of the experiment, as well as whenever zeta potential and particle size measurements are performed, in order to be able to plot the IEP (Isoelectric Point) of the measured nanoparticles and to keep track of possible changes in the sample. The monitoring of ph was achieved using the Orion™ 720Aplus pH-meter [35](Thermo Fisher Scientific, MA) (Figure 34), in combination with the glass electrode Orion™ 8156BNUWP[35] (Thermo Fisher Scientific, MA).

4.2 Manufacture of artificial seawater and f/2 medium

Since the same target organism will be used for this study (marine diatom *Thalassiosira pseudonana*), the realization of ASW and of f/2 medium is the same as the one already covered in Section 3.2

4.3 Nanoparticles

TiO_2 nanoparticles were extracted by two commercially available personal care products: sunscreen (Gardener's Armor™, Cincinnati, OH, 4% TiO_2, 4% colloidal oatmeal) and toothpaste (Colgate-Palmolive company, New York, NY, primary ingredients: 0.24% of sodium fluoride and TiO_2 as an inactive ingredient), both purchased from a local public store (Miami, FL).

The nanoparticles were then extracted from their respective products following the modified version of the protocol developed by Barker et al. (2008)[47]:

- Weight 3 g of product in a Falcon tube, using a precision scale,
- Add 30 mL of Hexane,
- Sonicate for 1 min and centrifuge at 4400 rpm for 5 minutes,
- Remove Hexane solution and add 30 mL of Ethanol,
- Centrifuge at 4400 rpm for 5 minutes,
- Discard the Ethanol solution,
- Add 30 mL of DI (ultrapure) water, shake manually for 2 minutes and then centrifuge at 3000 rpm for 10 minutes, then discard the supernatant; repeat this step two more times, and
- Place the open Falcon in the oven for 12 hours at a temperature of 100 °C,
- Put the Falcon in the desiccator.

Following the above procedure twice for each product, a sufficient amount of titanium dioxide (in the form of nano-powder) was obtained. In order to further refine the obtained nano-powders, they were grinded in sterilized manual grinders.

4.4 Diatom culture

The culture of the marine diatom *Thalassiosira pseudonana* was realized following the procedure illustrated in Section 3.4, and was preserved under the same environmental conditions: it was incubated at a constant temperature of 26°C, with 12h:12h (dark:light) cycles using the Verilux VT 10 white UV lamp illustrated in Section 3.1.3.

4.5 Experimental setup

In order to perform the designed growth inhibition tests, both the diatom culture and the TiO_2 nanoparticles were characterized in terms of absorbance, defining the peak absorbance wavelength for each of them. In fact, if the peak absorbance wavelengths of diatoms and nanoparticles were too close one to the other (i.e., enough to cause overlapping of absorbance peaks), the absorbance measurement would not have been a reliable indicator, and alternative ways to assess toxicity would have had to be found.

4.5.1 Detection of *T. pseudonana* peak absorbance wavelength

In the present study, several measurements of absorbance were performed on control samples and on samples that were exposed to TiO_2 nanoparticles under designated conditions. Absorbance was chosen as an indirect measurement of growth inhibition: the rationale behind this choice was that, under the condition that nanoparticles and diatoms had different and non-overlapping absorbance peaks, a lower absorbance in a contaminated sample would represent a decrease in diatom growth (i.e., growth inhibition), which has to be ascribed to the exposure to TiO_2 nanoparticles, since they are the only modification made with respect to the control sample.

The assessment of the peak absorbance wavelength has been explained in Section 3.5.1. Since this set of experiments used the same diatom (*Thalassiosira pseudonana*) as its target organism, the same peak absorbance wavelength, λ=674 nm was assumed for *Thalassiosira pseudonana.*

4.5.2 Product-derived nano-TiO_2 peak absorbance wavelength

As it was already stated in Section 3.5.2, the peak absorbance wavelength for TiO_2 nanoparticles is characterized by a great variability, influenced by multiple factors.

Since the nano-TiO_2 embedded in the toothpaste and sunscreen that were used this study will most likely differ from many of the titanium dioxide nanoparticles found in literature, it would have been unreasonable to assume a single value existing in literature.

Therefore, the same peak absorbance wavelength that has been used for industrial TiO_2 nanoparticles was also used for the product-derived TiO_2 nanoparticles, λ=350 nm.

4.5.3 Growth inhibition (%) as a function of exposure time

In this set of experiments, all of the tests were performed in triplicate copy, and different test samples were realized for toothpaste-derived TiO_2 nanoparticles and for sunscreen-derived TiO_2 nanoparticles. Test samples were prepared by adding 15 mL of colloidal suspension of TiO_2 in ASW + f/2 medium to 15 mL of diatom culture (see Section 3.4 for reference) into a 50 mL Petri dish. The control samples (also triplicate) were prepared by adding 15 mL of ASW + f/2 medium to 15 mL of diatom culture into a 50 mL Petri dish. After having gently mixed each sample, they were tested for absorbance (see section 3.1.1 for operational protocol). After the absorbance measurement, the samples were put in the incubator, under the conditions stated in Section 3.1.4.

Absorbance measurements were repeated at scheduled times: 5h, 12h, 24h, 48h, 72h, and 96h.

The concentration of toothpaste-derived and sunscreen-derived TiO_2 nanoparticles that were tested in this experiment was 5.0 mg/L.

The pH was measured at the beginning and at the end of the experiment using the pH-meter illustrated in section 3.1.4.

4.5.4 Growth inhibition (%) as a function of concentration

In this set of experiments, all of the tests were performed in triplicate copy, and different test samples were realized for toothpaste-derived TiO_2 nanoparticles and for sunscreen-derived TiO_2 nanoparticles. Each test sample was made by adding 15 mL of colloidal suspension of TiO_2 in ASW + f/2 medium to 15 mL of diatom culture (see Section 3.4 for reference) into a 50 mL Petri dish. The control samples (also triplicate) were prepared by adding 15 mL of ASW + f/2 medium to 15 mL of diatom culture into a 50 mL Petri dish. After having gently mixed each sample, they were tested for absorbance (see section 3.1.1 for operational protocol). After the absorbance measurement, the samples were put in the incubator, under the conditions stated in Section 3.1.4.

The samples were tested again for absorbance after a fixed elapsed time, t=72h.

The concentrations of toothpaste-derived and sunscreen-derived TiO_2 nanoparticles that were tested in this experiment were 1.0 mg/L, 2.5 mg/L, and 5.0 mg/L.

The pH was measured at the beginning and at the end of the experiment using the pH-meter illustrated in section 3.1.4.

4.5.5 Monitoring of particle size, zeta potential, and pH

Hydrodynamic particle size and zeta potential were measured at the beginning of the experiment and at time steps of 5h, 12h, 24h, 48h and 72h (the latter was previously assessed to be the break-through time), by using the Nano ZS90 zetasizer illustrated in Section 3.1.2, following the measurement protocol illustrated in the same section.

pH was measured at the beginning of the experiment and at time steps of 5h, 12h, 24h, 48h and 72h (the latter was previously assessed to be the break-through time), by using the OrionTM pH-meter illustrated in Section 3.1.4. The

measurements were performed by immersing the glass electrode in the sample, and then waiting for the stabilization before performing the reading of the current pH value.

All of the aforementioned measurements have been performed both on the control sample (see Section 3.5.3 for composition and preparation) and on the diatom cultures exposed to a 5 mg/L concentration of TiO_2 nanoparticles.

4.6 Results

4.6.1 Particle size, zeta potential, and pH

The measurements for all of the cultures exposed to 5 mg/L colloidal suspensions of industrial, toothpaste-derived, and sunscreen-derived TiO_2 nanoparticles are synthesized in Figure 5.3.

As it can be seen, in the case of toothpaste-derived TiO_2 nanoparticles a likely outliar is present at t=0h; neglecting it, it can be observed that particle size experienced a net increase during the exposure time, going from an initial size of 89 nm to a final size of 114 nm. Again, like in the case of industrial TiO_2, the particle size changed following a non-linear pattern, increasing until t=24h to a peak of 165 nm, and then decreasing sharply.

The surface charge was relatively low immediately after injecting the colloidal suspension, at a value of -4.56 mV. After 12h, however, it increased its absolute value up to -6.98 mV; from that time, it decreased its absolute value, reaching -5.37 mV at t= 48h; the value recorded at t=72h is most likely an outlier.

The measured value of pH decreased slightly and rather linearly during time, going from 8.48 to 7.39.

For sunscreen-derived TiO_2 nanoparticles, it can be seen that particle size experienced a net increase during the exposure time, going from an initial size of 46 nm to a final size of 92 nm. However, the particle size changed following a non-

linear pattern, increasing until t=24h to a peak of 100nm, and then decreasing linearly to the final value.

The surface charge was relatively low immediately after injecting the colloidal suspension, at a value of -5.89 mV. After 5h, however, it increased its absolute value significantly up to -7.95 mV; from that time, it decreased its absolute value, reaching -6.80 mV.

The measured value of pH decreased slightly and rather linearly during time, going from 8.47 to 7.32.

4.6.2 Growth inhibition (%) as a function of exposure time

The measured values of absorbance and the calculated values of growth inhibition will be shown in the following page. At each time, triplicate values of absorbance were recorded both for the control sample and for every other test sample. A statistical analysis was conducted on each triplicate experiment, computing statistically relevant parameters such as average, variance, standard error on mean (i.e., SEM), and performing the student *t*-test, in order to assess its statistical significance.

The average values were then used to compute growth inhibition, according to the correlation proposed by Cao et al. (2011)[45]:

$$GI\ (Growth\ Inhibition, \%) = \frac{\overline{abs_{control}} - \overline{abs_{sample}}}{\overline{abs_{control}}} \cdot 100$$

The absorbance values used in the calculation are the average for each triplicate set.

The statistical parameters that were computed for this set of experiments are, as anticipated:

- Standard deviation: this parameter allows to determine how disperse each triplicate set was. $\bar{x}$ represents the average for the triplicate set.

$$\sigma=\sqrt{\frac{\sum(x-\bar{x})^2}{(n-1)}}$$

- Standard error on mean (i.e., SEM): SEM is a measure of the precision of the mean.

$$SEM=\frac{\sigma}{\sqrt{n}}$$

- The student *t*-test was performed for all of the triplicate experiments, in order to assess their statistical significance. The test was conducted under the assumption of having two samples with equal variance. All of the tested concentrations showed statistical significance after t=96h (having $p<0.05$).

Following are the tables and plots summarizing the data, statistical analysis and results of the time-dependent toxicity test on toothpaste-derived and sunscreen-derived TiO_2 nanoparticles, at a concentration of 5.0 mg/L.

Table 4.1. Dataset and results for inhibition as a function of exposure time; toothpaste-derived nano-TiO2, 5.0 mg/L

concentration	5 mg/L						
time	0	5	12	24	48	72	96
control 1	0,020	0,023	0,021	0,027	0,044	0,083	0,104
control 2	0,022	0,023	0,020	0,024	0,044	0,080	0,098
control 3	0,023	0,020	0,019	0,023	0,045	0,079	0,104
AVG	0,022	0,022	0,020	0,025	0,044	0,081	0,102
ST DEV	0,002	0,002	0,001	0,002	0,001	0,002	0,003
SEM	0,001	0,001	0,001	0,001	0,000	0,001	0,002
TiO2 1	0,022	0,022	0,020	0,022	0,034	0,056	0,095
TiO2 2	0,026	0,020	0,018	0,021	0,036	0,052	0,088
TiO2 3	0,021	0,021	0,020	0,021	0,036	0,049	0,071
AVG	0,023	0,021	0,019	0,021	0,035	0,052	0,085
ST DEV	0,003	0,001	0,001	0,001	0,001	0,004	0,012
SEM	0,002	0,001	0,001	0,000	0,001	0,002	0,007
G.I. (%)	\	4,13	3,17	13,24	20,30	35,17	32,01
G.I. (%) ST DEV	\	4,51	3,88	2,48	1,14	1,36	0,24
G.I. (%) SEM	\	2,60	2,24	1,43	0,66	0,79	0,14

Table 4.2. Dataset and results for inhibition as a function of exposure time; sunscreen-derived nano-TiO2, 5.0 mg/L

concentration	5 mg/L						
time	0	5	12	24	48	72	96
control 1	0,020	0,023	0,021	0,027	0,044	0,083	0,104
control 2	0,022	0,023	0,020	0,024	0,044	0,080	0,098
control 3	0,023	0,020	0,019	0,023	0,045	0,079	0,104
AVG	0,022	0,022	0,020	0,025	0,044	0,081	0,102
ST DEV	0,002	0,002	0,001	0,002	0,001	0,002	0,003
SEM	0,001	0,001	0,001	0,001	0,000	0,001	0,002
TiO2 1	0,023	0,022	0,019	0,027	0,041	0,044	0,049
TiO2 2	0,022	0,020	0,021	0,020	0,028	0,035	0,038
TiO2 3	0,021	0,021	0,021	0,021	0,027	0,035	0,044
AVG	0,022	0,021	0,020	0,023	0,032	0,038	0,044
ST DEV	0,001	0,001	0,001	0,004	0,008	0,005	0,006
SEM	0,001	0,001	0,001	0,002	0,005	0,003	0,003
G.I. (%)	\	4,13	-2,00	8,45	27,73	52,98	57,27
G.I. (%) ST DEV	\	9,02	10,36	8,34	18,20	5,19	4,19
G.I. (%) SEM	\	5,21	5,98	4,81	10,51	3,00	2,42

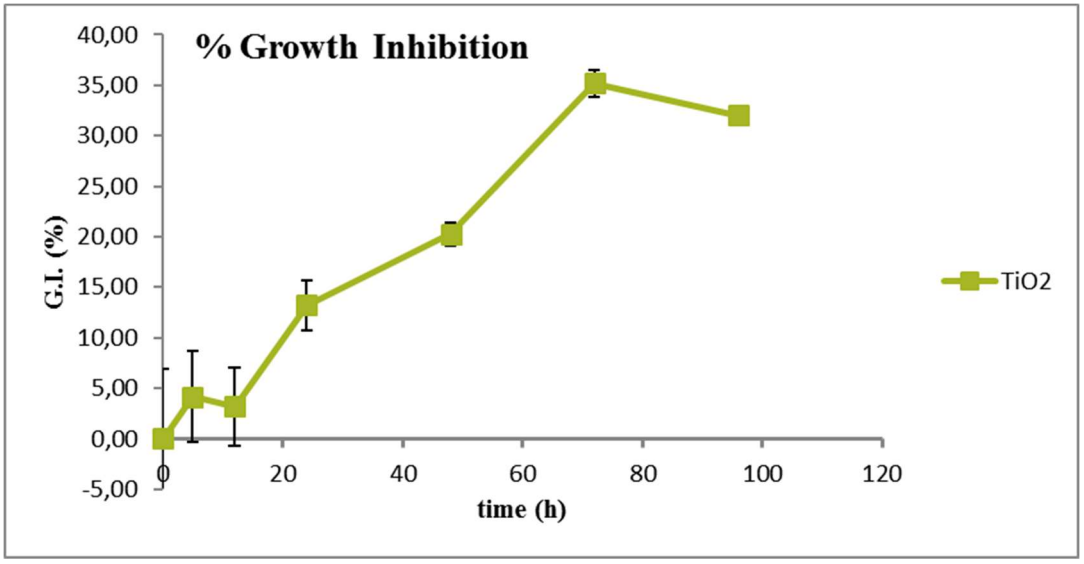

Figure 4.1. % Growth inhibition of *Thalassiosira pseudonana* exposed to toothpaste-derived TiO_2 nanoparticles, as a function of exposure time.

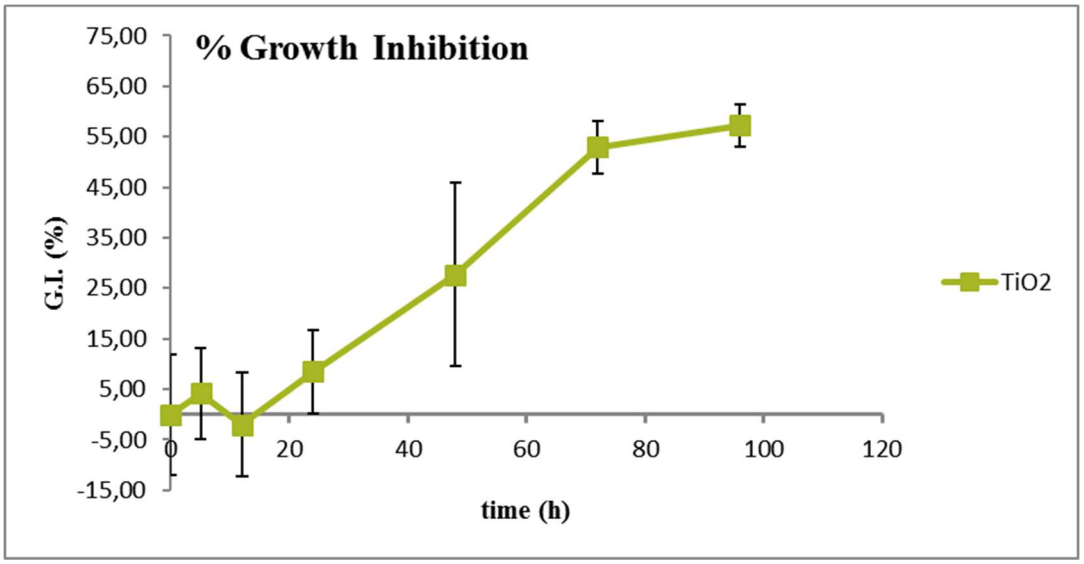

Figure 4.2. % Growth inhibition of *Thalassiosira pseudonana* exposed to sunscreen-derived TiO_2 nanoparticles, as a function of exposure time.

As it can be observed from both Figure 4.1 and Figure 4.2, a significant increase in % growth inhibition occurs after t=72h, while the preceeding growth inhibition is almost negligible and/or flawed by high standard deviations.

This can be explained again by comparing the growth inhibition curves with the typical cellular growth curve, shown in Figure 3.12: cellular growth is initially characterized by a lag-phase, during which almost no growth can be observed on the population.

The initially low growth inhibition is due to the fact that no diatom growth is likely to occur at all during the first phase, thus reducing the potential for growth inhibition.

Our plots have a strong resemblance with the first two phases of the cellular growth curve, that can be therefore used to justify the existence of a break-through time between 48h and 72h from inoculation (i.e. acceleration phase).

The experiments performed on toothpaste-derived and sunscreen-derived TiO_2 nanoparticles highlighted once again t=72h as the break-through point, confirming the findings of Section 3.6.2.

4.6.3 Growth inhibition (%) as a function of concentration

The measured values of absorbance and the calculated values of growth inhibition will be shown in the following page. At t=0h and t=72h (confirmed to be a proper break-through time in the previous section), triplicate values of absorbance were recorded both for the control sample and for every other test sample. A statistical analysis was conducted on each triplicate experiment, computing statistically relevant parameters such as average, variance, standard error on mean (i.e., SEM), and performing the student *t*-test, in order to assess its statistical significance.

The average values were then used to compute growth inhibition, according to the correlation proposed by Cao et al. (2011)[45]:

$$GI\ (Growth\ Inhibition, \%) = \frac{\overline{abs_{control}} - \overline{abs_{sample}}}{\overline{abs_{control}}} \cdot 100$$

The absorbance values used in the calculation are the average for each triplicate set.

The statistical parameters that were computed for this set of experiments are, as anticipated:

- Standard deviation: this parameter allows to determine how disperse each triplicate set was. $\bar{x}$ represents the average for the triplicate set.

$$\sigma = \sqrt{\frac{\sum(x-\bar{x})^2}{(n-1)}}$$

- Standard error on mean (i.e., SEM): SEM is a measure of the precision of the mean.

$$SEM = \frac{\sigma}{\sqrt{n}}$$

- The Pearson Correlation Coefficient was computed for concentration versus percent growth inhibition.

$$r = \frac{\sum[(conc - \overline{conc})(G.I. - \overline{G.I.})]}{\sqrt{\sum[(conc - \overline{conc})^2 (G.I. - \overline{G.I.})^2]}}$$

The computed correlation coefficient between concentration and percent growth inhibition for toothpaste-derived and sunscreen-derived TiO_2 nanoparticles are respectively equal to 0,994 and 0,959, thus showing a rather strong positive correlation between the aforementioned parameters.

Following are the tables and plots summarizing the data, statistical analysis and results of the concentration-dependent toxicity test performed on toothpaste-derived and sunscreen-derived TiO_2 nanoparticles, at the concentrations of 1.0 mg/L, 2.5 mg/L, and 5.0 mg/L.

Table 4.3. Dataset and results for inhibition as a function of concentration at breakthrough time t=72h.

Sample	abs (t=0h)	abs (t=72h)	G.I. (%)	G.I. (%) ST. DEV	G.I. (%) SEM
Control 1	0,010	0,030			
Control 2	0,010	0,028	/	/	/
Control 3	0,009	0,023			
Toothp. TiO2 1mg/l #1	0,012	0,022			
Toothp. TiO2 1mg/l #2	0,010	0,023	18,519	0,540	0,312
Toothp. TiO2 1mg/l #3	0,011	0,021			
Sunscr. TiO2 1mg/l #1	0,013	0,016			
Sunscr. TiO2 1mg/l #2	0,013	0,017	39,506	0,146	0,084
Sunscr. TiO2 1mg/l #3	0,010	0,016			
Toothp. TiO2 2.5mg/l #1	0,010	0,024			
Toothp. TiO2 2.5mg/l #2	0,009	0,020	22,222	1,191	0,687
Toothp. TiO2 2.5mg/l #3	0,010	0,019			
Sunscr. TiO2 2.5mg/l #1	0,010	0,015			
Sunscr. TiO2 2.5mg/l #2	0,010	0,015	45,679	0,126	0,073
Sunscr. TiO2 2.5mg/l #3	0,009	0,014			
Toothp. TiO2 5mg/l #1	0,010	0,020			
Toothp. TiO2 5mg/l #2	0,009	0,020	32,099	0,899	0,519
Toothp. TiO2 5mg/l #3	0,010	0,015			
Sunscr. TiO2 5mg/l #1	0,010	0,013			
Sunscr. TiO2 5mg/l #2	0,009	0,014	49,383	0,117	0,068
Sunscr. TiO2 5mg/l #3	0,010	0,014			

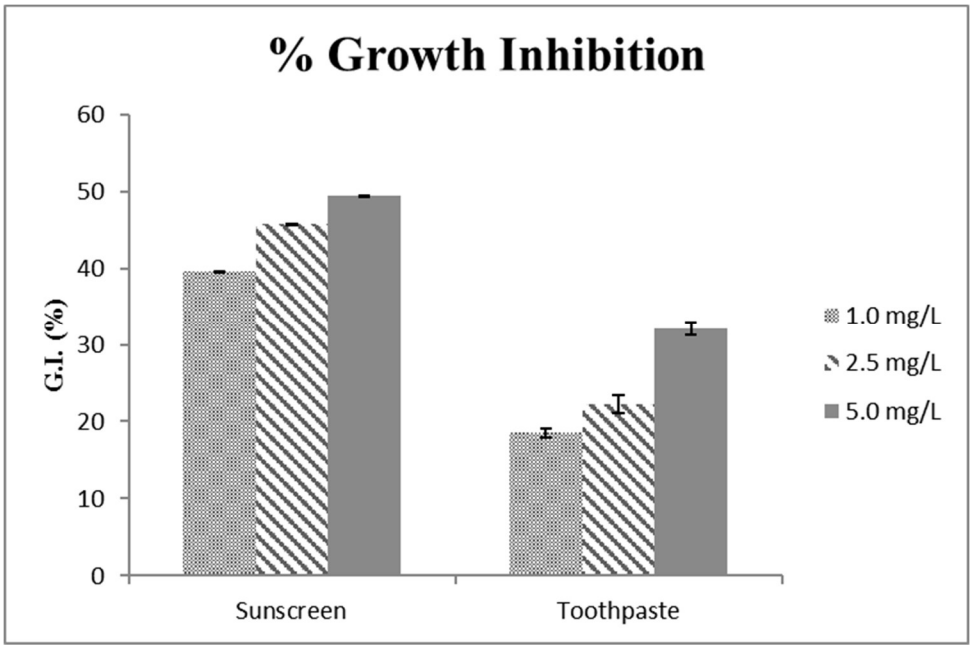

Figure 4.3. % Growth inhibition of *Thalassiosira pseudonana* as a function of concentration of sunscreen-derived and toothpaste-derived TiO_2 nanoparticles at break-through time t=72h.

Chapter 5 - Comparison of results and discussion

Several sets of experiments were performed in order to assess the toxicity of different types of TiO_2 nanoparticles (industrial, toothpaste-derived, and sunscreen-derived) to the marine diatom *Thalassiosira pseudonana*.

The parameters that were taken into account to evaluate the toxic effects of TiO_2 nanoparticles are:

- Exposure time: the duration of the time interval during which the samples were exposed to TiO_2 nanoparticles. In order to highlight the role of exposure time, the experiments were performed at fixed concentrations, in order to have one less variable involved,
- Concentration: the amount of TiO_2 nanoparticles, expressed in mg/L that were inoculated in the test samples. This set of experiments was performed once the break-through time for each particular TiO_2 nanoparticle had been assessed through the first set of experiments. Dose-dependent growth inhibition tests were performed at a constant exposure time equal to the break-through time, in order for the concentration to be the only variable involved,
- Hydrodynamic particle size: the particle size of the tested samples detected by the zetasizer. Its variations can clarify the relevance physically-based toxicity mechanisms such as aggregation or surface adsorption,
- Zeta potential: the surface charge on the particles detected by the zetasizer. Knowing the surface charge of the particles, it is possible to explain their behavior in accordance to colloidal chemistry,
- pH: the pH of the solution has implications in its stability, and was therefore monitored.

The experiments were run and analyzed separately for industrial TiO_2 nanoparticles and for product-derived TiO_2 nanoparticles. In the following pages the results of all of the performed experiments and measurements will be compared, in order to get a better understanding on what influence the aforementioned parameters

and most importantly nanoparticles' nature can have in the toxic effect of TiO_2 nanoparticles toward the marine diatom *Thalassiosira pseudonana*.

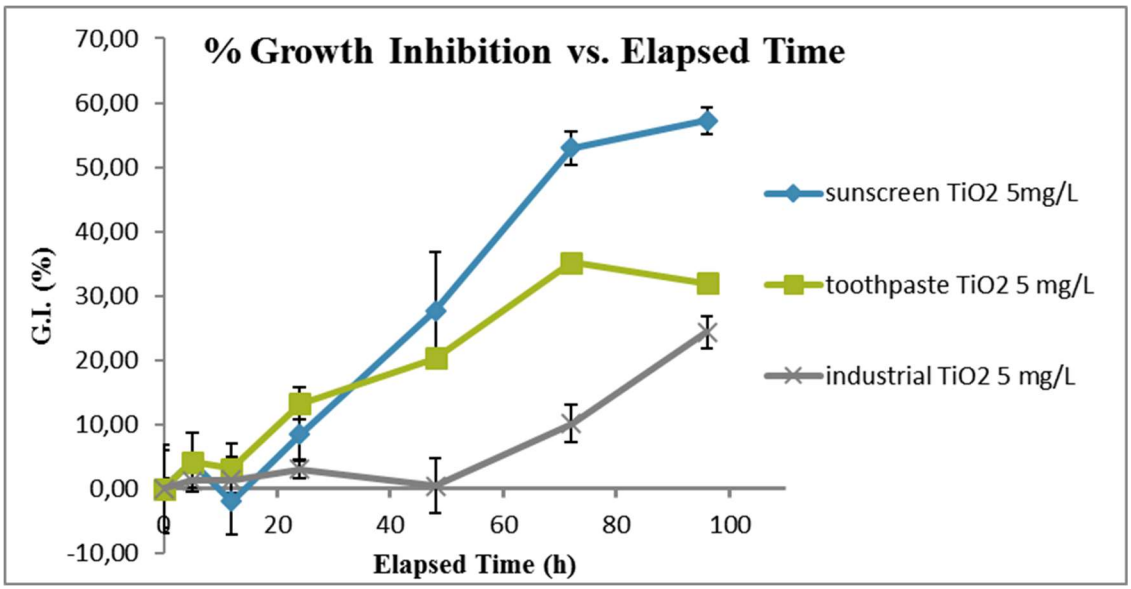

Figure 5.1. % Growth inhibition as a function of the elapsed time for all of the three types of titanium dioxide at a constant concentration of 5 mg/L.

In Figure 5.1 are summarized the results of all of the time-dependent growth inhibition tests (except for the one regarding industrial TiO_2 nanoparticles at a concentration of 2.5 mg/L, that is not being considered because it had a different concentration and control sample, and would therefore be inconsistent for this comparison).

As it can be seen from the above plot, until t=48h the measured growth inhibitions are highly deviated and negligible when compared to the latter values. As it has already been mentioned in Sections 3.6.2 and 4.6.2, this is most likely due to the initial lag phase through which the all the samples went. During this period of time, cellular growth is almost zero, and therefore the computation of % values makes the numbers look highly inconsistent and variable, as they effectively are.

However, at t=48h all of the tested samples have gone through the initial lag phase, and by t=72h the different toxic behaviors can be observed fully.

From our interpretation of the results, sunscreen-derived TiO_2 nanoparticles resulted the most toxic to the target specie, followed by toothpaste-derived TiO_2 nanoparticles, showing that industrially produced TiO_2 nanoparticles have the least toxic effects as a function of the elapsed time.

All of the TiO_2 nanoparticles showed a direct proportionality between growth inhibition and elapsed time.

As a conclusion, it can be said that these factors were found to inhibit the growth of *Thalassiosira pseudonana* when exposed to TiO_2 nanoparticles:

- Exposure time directly influences growth inhibition: the longer the exposure time, the higher the growth inhibition. Growth inhibition occurs in significant amounts only when the exposure time exceeds a break-through point which is specific to every nanoparticle,
- The nature of the TiO_2 nanoparticles strongly influences the growth inhibition: sunscreen-derived TiO_2 nanoparticles caused the highest growth inhibition, while the lowest effect was caused by industrially produced TiO_2 nanoparticles.

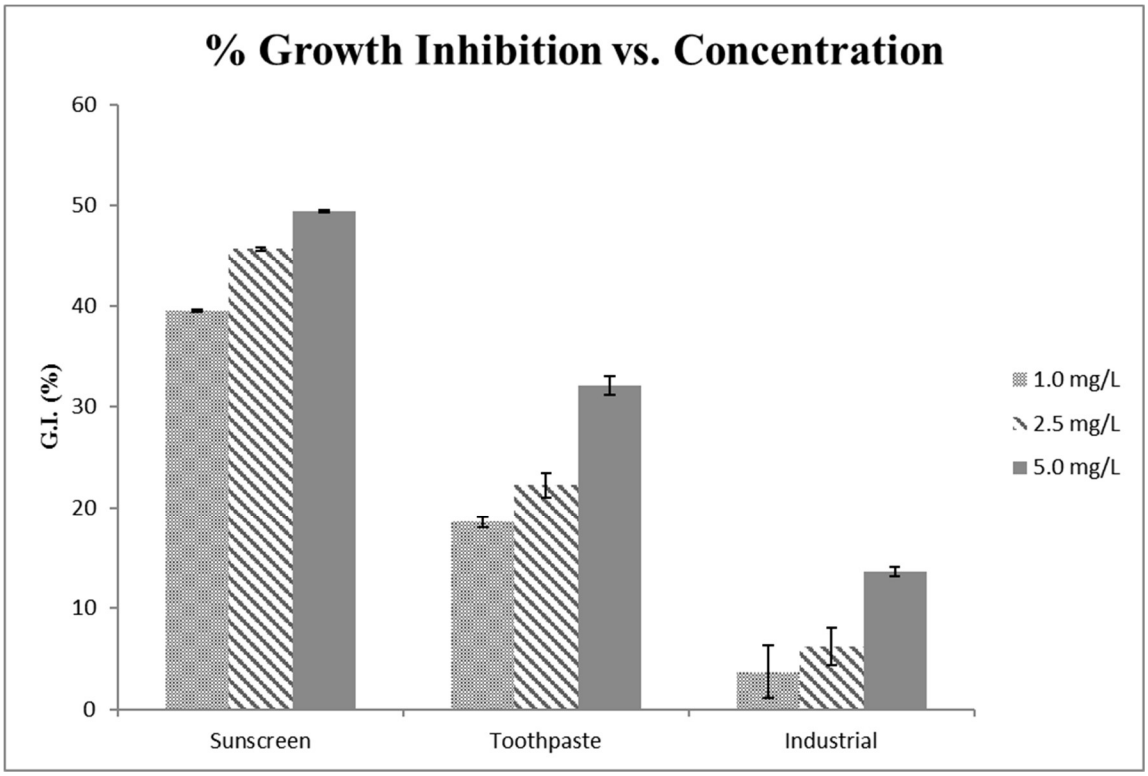

Figure 5.2. % Growth inhibition as a function of the nanoparticle concentration for all of the three types of titanium dioxide, at a constant exposure time t=72h.

In Figure 5.2 are summarized the results of all of the concentration-dependent growth inhibition tests, performed at a fixed exposure time equal to 72h.

The above plot shows the different growth inhibition effects exhibited from TiO_2 nanoparticles of different nature, at the tested concentrations of 1.0 mg/L, 2.5 mg/L, and 5.0 mg/L.

From the plot it can be deducted that growth inhibition caused by TiO_2 nanoparticles is related to the concentration of nanoparticles provided. The proportionality between percent growth inhibition and TiO_2 nanoparticles concentration can be regarded as barely linear, allowing some variability due to the complex nature of the phenomenon that is being analyzed.

Moreover, it is very clear from the plot that the conclusions drawn from the set of time-dependent experiments are correct: in fact, sunscreen-derived TiO_2

nanoparticles caused the highest growth inhibition, while the lowest effect was caused by industrially produced TiO_2 nanoparticles in the set of concentration-dependent experiments, exactly like it happened in the former group of experiments.

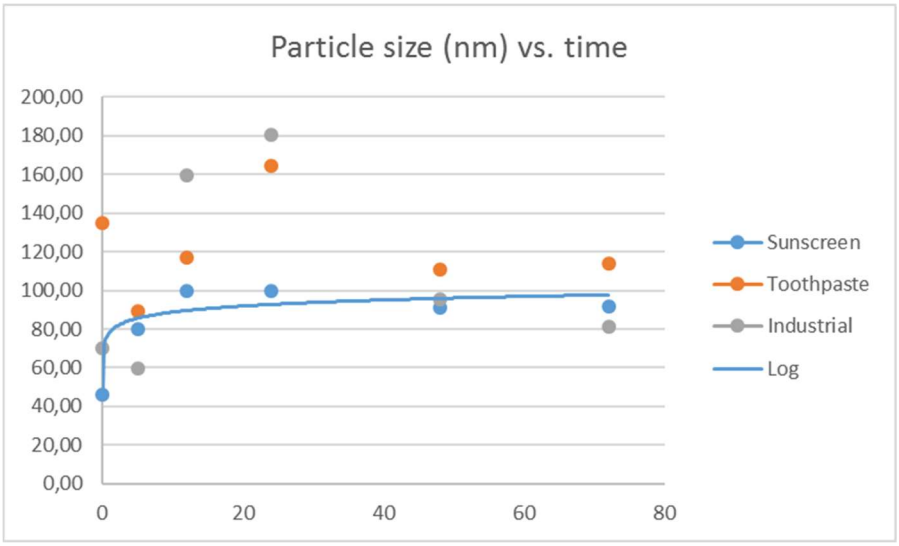

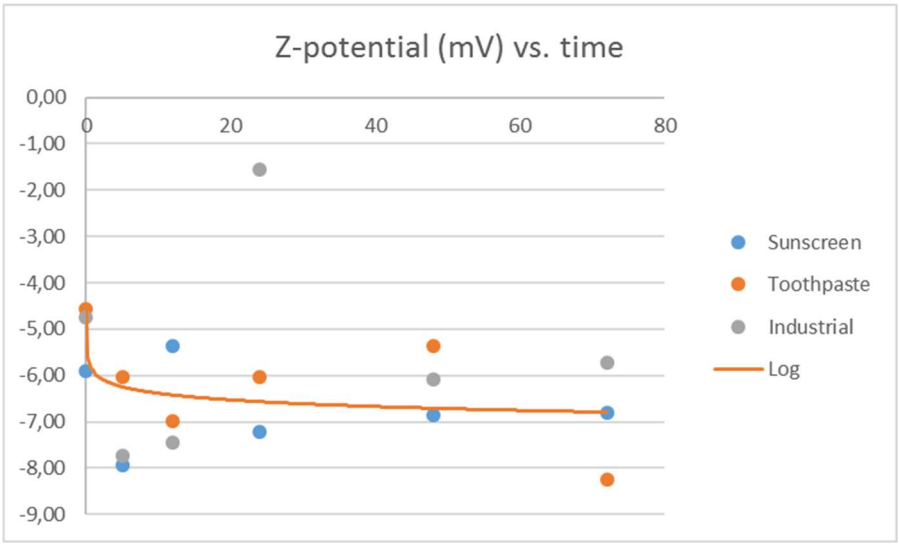

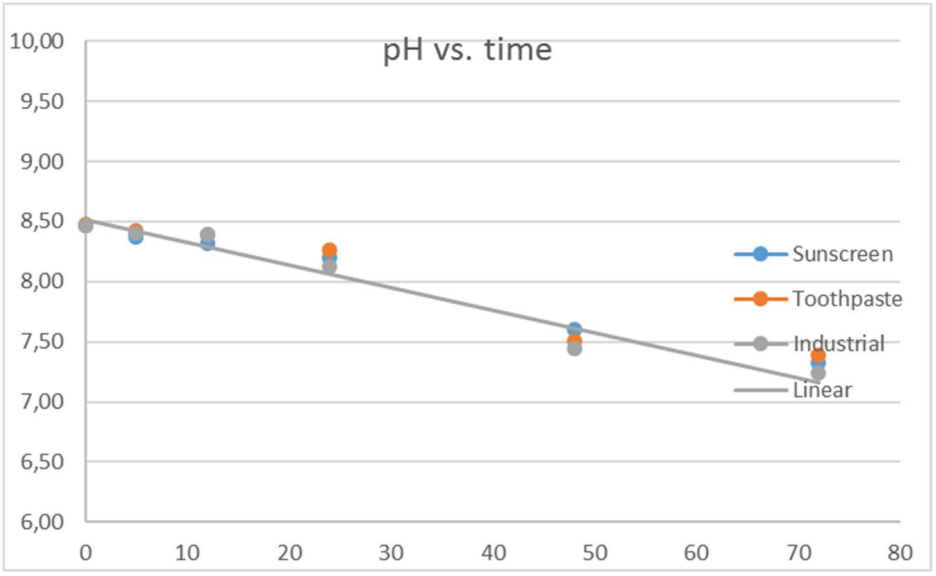

Figure 5.3. Hydrodynamic particle size, zeta potential and pH of TiO2 in 72 hours [breakthrough point] of exposure to *T. pseudonana* [TiO2 suspensions concentration: 5 mg/L]. (Galletti and Seo et al., 2016, submitted)

In Figure 5.3 are summarized the results of all of the monitoring of particle size, zeta potential, and pH, performed on all the samples exposed to TiO2 suspensions at a concentration of 5 mg/L, performed at the beginning of the experiment and at the assessed breakthrough time, equal to 72h.

From the plot it can be seen that the increase in hydrodynamic particle size is consistent with the measured toxicity, as sunscreen-derived TiO2 nanoparticles experienced the largest increase in size, while industrial TiO2 nanoparticles showed the lowest size. Given this result, aggregation appears as a possible mechanism for the macroscopic observed inhibitory effects. The increase in particle size finds further justification in the other almost-favorable environmental conditions that were monitored, such as pH and surface charge; in fact, it has been reported that decreasing values of pH tend to favor the aggregation of nanoparticles[48]; moreover, the measured values of pH were getting closer to the IEP (point of neutral surface charge), and this was confirmed from the decreasing values of zeta potential that were measured.

The aforementioned environmental conditions might explain the aggregation behavior. However, it was also reported that the presence of negatively charged

NOM (natural organic matter)[49] tends to impair the aggregation of TiO2 nanoparticles, as well as the fact that if particles (diatom and TiO2) have a surface charge of the same sign, they will naturally tend to repel, rather than attract, each other. Nonetheless, the observed particle sizes are consistent with the reported levels of inhibition, and aggregation can better explain SEM images, where the diatom cells were found to be destroyed at the end of the experiment (possibly grinded by aggregating TiO2 nanoparticles).

The following conclusions can be drawn from all of the performed analyses:

- Exposure time directly influences growth inhibition: the longer the exposure time, the higher the growth inhibition. Growth inhibition occurs in significant amounts only when the exposure time exceeds a break-through point which is specific to every nanoparticle,
- Concentration of TiO_2 nanoparticles directly influences growth inhibition: the higher the concentration, the higher the observed growth inhibition. This relationship also shows a weakly linear trend,
- Particle size experienced the highest increase in sunscreen-derived TiO2 nanoparticles, consistently with the values of growth inhibition reported in the other experiments, thus suggesting aggregation as a possible toxicity mechanism,
- Zeta potential and pH marginally explain and confirm the observed aggregation, according to the existing literature; nonetheless, it has to be noted that electrostatic interactions tend to be weaker than mechanical interactions, especially at increasing particle sizes. Therefore, the impact of these two parameters might have been only of secondary magnitude in the aggregation kinetics, and
- The nature of the TiO_2 nanoparticles strongly influences the growth inhibition: sunscreen-derived TiO_2 nanoparticles caused the highest growth inhibition, while the lowest effect was caused by industrially produced TiO_2 nanoparticles in all of the performed experiments.

The last point is a really encouraging result, as the research activity on product-derived TiO_2 nanoparticles is currently in its early stages, especially in the field of toxicity to marine environment. This result demands further research to clarify the driving toxicity mechanisms that acted behind it.

Chapter 6 - Literature survey

In the present study, growth-inhibition tests aimed to the assessment of the toxic effects of industrial-, sunscreen-, and toothpaste derived TiO_2 nanoparticles, were performed exposing the marine diatom *Thalassiosira Pseudonana* to suspensions of nano-TiO2, varying the concentration, the exposure time, and the nature of the TiO2 NPs used. As a result, a dose-dependent response was observed in all samples, showing the most significant toxicity effects after a break-through point found at around t=72h. in particular, titanium dioxide nanoparticles derived from commercially available sunscreen were the most toxic to the targeted organism, followed by titanium dioxide derived by toothpaste, being the industrially available TiO2 NPs (Sigma Aldrich)[39] the ones showing the least toxic effects.

A literature survey showed that toxicity mechanisms such as photo activity followed by ROS (Reactive Oxygen Species) production and induced oxidative stress, surface adsorption followed by membrane disruption mechanisms, and membrane piercing due to shape and size, could be involved in the macroscopic toxic effects that were observed, and that various environmental conditions might influence the toxicity exerted by the nanoparticles. Finally, it seems rather obvious that toxic effects cannot be ascribed to single factors alone, but rather to a combination of them. For instance, the salinity of the test environment together with the measured pH=8.0 are likely to have prevented (or at least impaired) aggregation (see section 6.1.1), thus making it an unlikely toxic mechanism despite the colloidal properties of the suspension. Another example is the effect of UV irradiation that, despite allowing a regular photosynthetic activity, enables the photoactive properties of anatase TiO_2, ultimately resulting in an increased toxicity.

As a result, the following survey was carried over, in order to provide a better understanding of the single toxicity mechanisms that took place in our experiments, as well as to provide a base to discuss their possible interactions.

The survey highlighted many different parameters that play primary and marginal roles in the toxic effects of nano-TiO_2, that is possible to distinguish and classify as:

- Environmental parameters: parameters belonging to this category have the possibility to enhance or reduce the toxic effect of the nanoparticles. In fact, the environment can have both synergistic or inhibiting effects towards toxicity, depending on its conditions.

- Physical and chemical parameters: these parameters reflect properties of the nanoparticles that influence directly or indirectly their toxicity. Toxicity is influenced by these parameters as they are, since the toxic effects they exert are led by physical and chemical laws.

- Biological parameters: parameters belonging to this category describe the effective uptake, and therefore possible exposure, of nanoparticles from a certain organism. It is important to define the biological parameters in order to know the likelihood of the risk that the other two categories of parameters predict.

6.1 Environmental parameters

Among the environmental factors are all of those factors that are not a direct property of the nanoparticles, nor a biological parameter related to the target organism. In the following subsections those who are the main environmental parameters in the nanoparticle-diatom interaction will be highlighted, in an attempt to clarify their influence on the nanoparticles' toxicity in the present case of study.

6.1.1 Ionic strength

An important environmental factor in the assessment of the potential toxic effects of a nanoparticle is the ionic strength of the medium in which the observation takes place. Ionic strength is the overall concentration of (all) the ions in a solution, and is measured in M (mol/L); therefore, it gives a measure of the remaining amount of ions that can be released in a certain solution.

French et al. (2009)[50] demonstrated that increasing the ionic strength of the test solution while maintaining the pH constant, led to the formation of micro-scaled TiO_2 aggregates in a relatively short time (15 minutes).

It was shown by Chambers et al. (2013)[51] that Ag nanoparticles lose stability when the ionic strength of the solution is increased, with a tendency to form aggregates. On the other hand, the effects of different concentrations of chloride were tested, and it was found that chloride acts as a stabilizer, favoring the formation of AgCl particles and letting them aggregate with Ag NPs in lieu of other Ag NPs. In the same study, it was found that differences in ionic strength do not significantly influence the solubility of Ag NPs, with the first only showing after 10 minutes. In the same study the fractal dimension (an inverse index of the number of particles per unit volume) of the nanoparticles was investigated: the findings highlighted how an increased ionic strength would cause a decrease of the fractal dimension, meaning that a larger specific surface area was available; this result was further confirmed by an increased toxicity for higher ionic strength.

In the present case of study, artificial seawater[37] was used and, despite the ionic strength was not measured, usual values of chloride in seawater are around 20,000 mg/L. the chloride concentrations tested by Chambers et al. ranged from 0 to around 6,000 mg/L[51], and the effects of chloride were already not only visible, but even dominant.

As it can be seen from Figure 6.1 a higher chloride concentration caused bridging between nanoparticles, actually reducing their chemical availability and toxicity by reducing their specific surface area (the impact of which will be covered later).

Therefore, it can be inferred that chloride presence in our case of study has had relevant influence on the toxic effects exerted from TiO_2 nanoparticles, contributing to their aggregation and reducing their overall toxic effect.

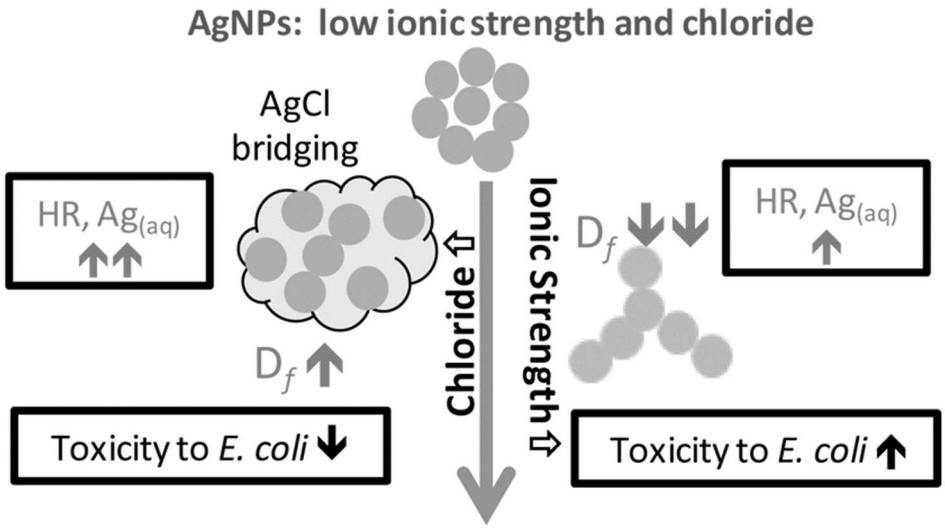

Figure 6.1. Effects of chloride and ionic strength on the toxicity of silver nanoparticles.[51]

6.1.2 Environment pH

pH is an important environmental parameter that should be considered whenever an aqueous medium is studied, as it gives a measure of the chemical aggressiveness of said medium. If pH happens to be outside a certain range, the dissolution of the nanoparticle or, conversely, its complexation with other materials might be enhanced, thus influencing the toxic behavior of a metal oxide nanoparticle.

Waalewijn-Kool et al. (2013)[52] investigated the effects of soil's pH on the toxicity of ZnO NPS towards the arthropod *Folsomia candida*, testing three different levels of pH (4.31, 5.71, and 6.39).

According to their findings, sorption of Zn increased with increasing pH, as well as Freundlich constants K_f increased, indicating an enhanced sorption capacity. Particle size was shown not to have a significant impact on sorption, as nanoparticles of different size (30 nm and 200 nm) and salt $ZnCl_2$ were tested with negligible discrepancies in the results. Particle size was also found to influence the overall toxicity of ZnO towards *Folsomia Candida* just in a marginal way. Their study assessed ZnO NPS to be more toxic towards the targeted organism when they were tested in a more acidic soil, rather than a less acid one.

The results also highlighted that the explanation for toxicity is most likely the speciation of Zn with Ca (present in the soil samples), rather than the physical hazard posed by the nanoparticles, since pH plays a key role in the solubility of ZnO and in its consequent biological and chemical availability.

Another relevant result was obtained by Seitz et al. (2015)[53], who studied the effects of pH in combination with the presence or the absence of dissolved organic matter. The toxicity of silver nanoparticles (nAg) against *Daphnia Magna* was measured by Seitz et al. (2015) under two different values of pH (6.5 and 8) and in presence and absence of dissolved organic matter. The results highlighted that a lower pH generally leads to a more toxic behavior, although the presence of dissolved organic matter can reduce said toxic effects up to 50%; similar results were obtained both in the acute toxicity and long-term toxicity tests. Both studies highlighted the interactions that might occur between metal oxide nanoparticles and the surrounding environment, how different levels of pH influence different kinds of interaction, ultimately impacting the toxicity of the nanoparticles to the target organism, either increasing or decreasing it.

Our experiments were performed at an initial pH = 8.0, which later decreased slightly to not less than 7.5 in all experiments, which is fairly different from the known IEP of nano-TiO_2 (reported[25,54] to be near 6.0 for anatase-type nano-TiO_2). Under such conditions, the aggregation of the nanoparticles should be impaired, and therefore the toxic effects associated to it cannot be ascribed to the environmental pH. Based on this, pH is not likely to have had a major impact on the toxicity measured in our experiments, yet being an important environmental factor to consider for its implications in secondary chemical reactions.

6.1.3 Light irradiation

It has been shown in numerous works that exposure to daylight (and thus, to UV radiation), acts as a strong activator for many nanoparticles; in fact, many tests performed under permanent dark conditions assessed that no toxic effect was produced by TiO_2 nanoparticles.[21,55]

The present study has been performed in order to reproduce usual environmental conditions found in the marine environment, therefore a light cycle of 12 hours was used for all of the experiments.

Despite the fact that experiments under permanent darkness condition were not performed in the present study, light radiation might have, in accordance with all of the existing literature, acted as a catalyzer and favored photochemical reactions that might have exerted toxicity (they will be treated in detail under the "Photo-activity and ROS Production" subsection).

6.2 Physical and chemical parameters

Physical and chemical parameters are those properties that belong exclusively to the nanoparticle, and therefore will obey certain natural laws regardless of the organisms that are tested or of the environment in which the experiment takes place.

It is therefore important to be aware of the nature of the nanoparticles that we are dealing with because, as it will be shown in the following subsections, some of their traits have a primary relevance in their toxic effects towards the target organism.

6.2.1 Colloidal properties

Metal oxide nanoparticles do not usually dissolve in aqueous solution, mostly forming colloidal suspensions. Colloids are dispersed systems in which two phases are present: the first phase is an insoluble substance present in nano-sized particles (dispersed phase), and it is suspended in one second fluid phase acting as a medium (continuous phase).

Chen et al. (2010)[56] studied the interactions of colloidal solutions with the nearby environment; ultimately, the stability of colloids was measured and compared to the physical and chemical properties of their constituents. The stability of a colloid is ultimately reflected by the state of aggregation and by the deposition trend of the dispersed phase, eventually resulting in sedimentation; the more stable a solution is, the less aggregation it will experience.

Aggregation is caused by Brownian motion of particles into the continuous phase, until they become very close to each other; at small intermolecular distances, electrostatic repulsion loses effectiveness, and aggregation is driven by short-ranged interaction forces. Such forces are the Wan der Waals interactions and the electric double layer interactions; according to DLVO theory, the attractive or repulsive force between particles comes as the sum of these two interactions. Wan der Waals interaction strength is a molecular-level interaction based on the colloid's chemistry, while electric double layer interactions depend are electric-based forces depending on the colloid's pH and ionic strength.

As it is shown in Figure 6.2, the separation of nanoparticles in a colloidal solution can occur both due to Wan der Waals interactions and electrostatic repulsion. Therefore, it is important to know the chemistry of the solution as well as the environmental parameters involved in the experiment, in order to be able to control the aggregation level of the colloid.

In our case of study, no stabilizers were used and therefore no change in aggregation is to be expected. Moreover, the environmental pH was measured to be equal to 8.0 throughout the experiments, which is different from reported[25,54] values of IEP for anatase-phase nano-TiO_2 (usually around 6.0). Therefore, aggregation is not likely to have taken place during this study.

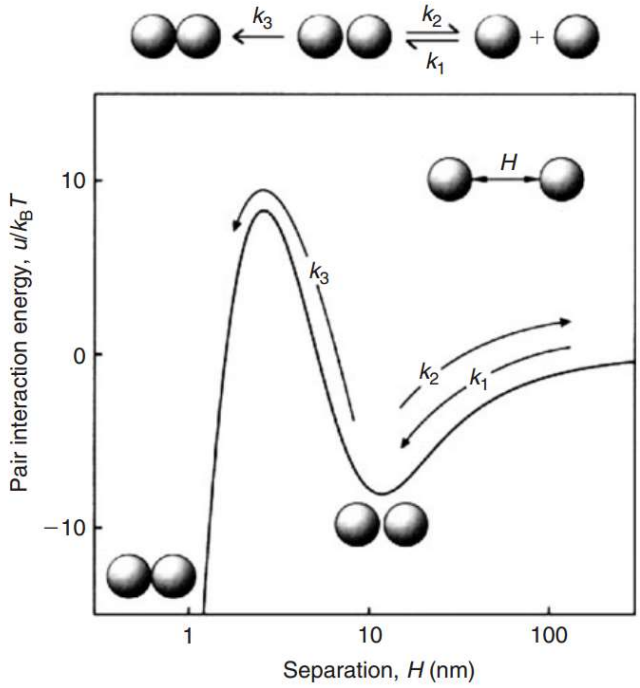

Figure 6.2. Relationship between interaction energy and nanoparticles' spacing.[56]

6.2.2 Zeta potential and isoelectric point

Zeta-potential is the measure of the charge on a colloidal particle's surface. In particular, it measures the electrostatic force between the particle and the fluid in which it is suspended, ultimately giving information on the aggregation state of the colloid and on its stability.

Patil S. et al (2007)[57] have inspected the effects of zeta-potential on cerium oxide NPs, with respect to protein adsorption and on cellular uptake. The targeted protein was BSA (bovine serum albuminum), while the cells tested for uptake were A549, namely adenocarcinoma lung cells. Two different preparation techniques were used to prepare a colloidal suspension of CeO_2 NPs: microemulsion and hydrothermal process. The two processes yielded different suspensions: the first had a primary particle size of 3-5 nm, zeta potential of -16.24 mV and I.E.P. (isoelectric point, a specific pH value at which particles show no charge) of roughly 4.5, while the second colloid had a primary particle size of 8-10 nm, zeta-potential of 33.60 mV and I.E.P. at pH 9.5. the reason for these discrepancies is in the preparation process: while in the first process NH_4OH is used (alkaline), the second preparation makes

use of HCl. Thus, the different chemical and physical properties of the colloids. Protein adsorption was higher in hydrothermal CeO_2 (positive zeta-potential), mainly due to the I.E.P. of BSA: at its I.E.P. (i.e., pH 4.78), BSA is hydrophobic, while at higher pH (like in aqueous solutions at neutral pH), it becomes negatively charged, and therefore attracts positively charged particles more. However, other mechanisms can be argued in order to justify the higher absorption onto positively charged nanoparticles; for instance, the dispersion of hydrothermal CeO_2 NPs could be more stable at higher pH, thus ensuring a greater effective surface area for adsorption, yet electrostatic interactions remain the leading cause.

Schwegmann et al. (2010)[58] analyzed the effects of zeta potential on the sorption of iron oxide. The target organisms were *S. cerevisiae* and *E. coli*, as representatives of *Prokaryotes* and *Eukaryotes*. The sorption on both organisms was well fitted by a Langmuir isotherm, showing the formation of a monolayer upon sorption. Under higher attraction conditions (lower zeta potential) the surface of the target microorganisms was largely covered with nanoparticles. However, at higher pH (10) no bactericidal effect was observed, in contrast with the strong bactericidal effect observed on E. coli at pH=4. The bactericidal effect is apparently related to the level of sorption, which ultimately relates to the electrostatic forces. Since mainly individual particles or small aggregates were sorbed, it was argued that the bactericidal effect was partially due to the particle size, in accordance with Roiter et al. (2008)[59], who found that particles in the range of 1-22 nm can pierce the cell membrane, leading to cellular death. Despite being indirect, the link between zeta potential and possible toxicity of nanoparticles is again clear.

As for cellular uptake, Patil S. et al (2007)[57] registered the highest values for microemulsion CeO_2 NPs, which had the lowest (negative) zeta potential, and smallest particle size among the two, and uptake came as a second step after surface adsorption. Since it is well known that cells possess many negatively charged domains, it could be argued that the highest uptake happens with positively charged particles. However, experimental data proved the opposite, thus proving the existence of minor positively charged domains on cells, onto which negatively charged nanoparticles can adsorb.

It was also suggested from Wilhelm et al. (2003)[60] that nanoparticles adsorb onto cellular cationic sites in clusters, due to the high repulsion exerted by the other anionic domains, also showing that adsorbed particles have lower charge density, easing the adsorption of other particles; once adsorbed, nanoparticles enter the cell through different mechanisms (pinocytosis, i.e., the mechanism through which small particles are brought into the cell, forming an invagination in the membrane, and then suspended within small vesicles, and endocytosis, an active process during which the cell depletes energy to engulf a small particle (usually, proteins)).

As it can be seen in Figure 6.3, the Isoelectric Point of TiO_2 nanoparticles is not fixed, it rather varies slightly according both to pH and to the nanoparticles' nature. Except pure rutile-phase TiO_2, all of the other titania have their Isoelectric Point near pH=6. In the present case of study, since all of the experiments were performed at a starting pH=8.0 that remained above 7.5 throughout the experiment, negative zeta potential is to be expected in the test environment. As a consequence, the negative zeta potential of the solution will not allow nanoparticles to aggregate, therefore remaining suspended and available for biological uptake by *Thalassiosira pseudonana*.

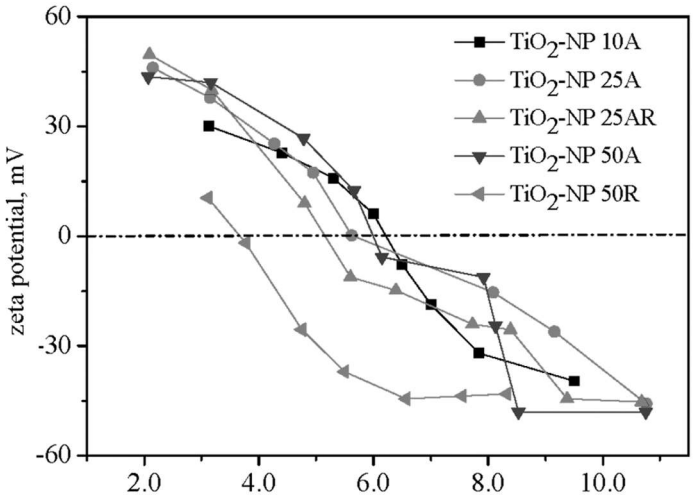

Figure 6.3. Isoelectric Point as a function of pH for titanium dioxide nanoparticles of different nature.[25]

6.2.3 Particle size and specific surface area

Particle size is almost never found as a deterministic value when dealing with nanoparticles. Rather than that, it is more likely that particle size is distributed through a certain PDF (probability density function). The size with the highest probability density is called primary particle size, and it is the one usually took into account for toxicity studies.

Lin et al. (2014)[25] found that smaller particles have larger BET area (i.e., Brunauer-Emmett-Teller area, a theory based on the quantification of surface adsorption onto multiple layers), and larger hydrodynamic diameter. The smaller the particle size, the larger the magnification of many physical-chemical properties (i.e., optic properties, atomic reactivity, electronic reactivity, surface activity, surface-to-mass ratio, etc.). As it can be seen from Figure 6.4, experiments conducted on TiO_2 nanoparticles of different size and nature, highlighted that smaller nanoparticles are more chemically active, and for instance produce more ROS (Reactive Oxygen Species) and MDA (malondialdehyde) compared to larger nanoparticles. Chemical availability is often recognized as an indirect measure of the potential toxic effects that one nanoparticle could have.

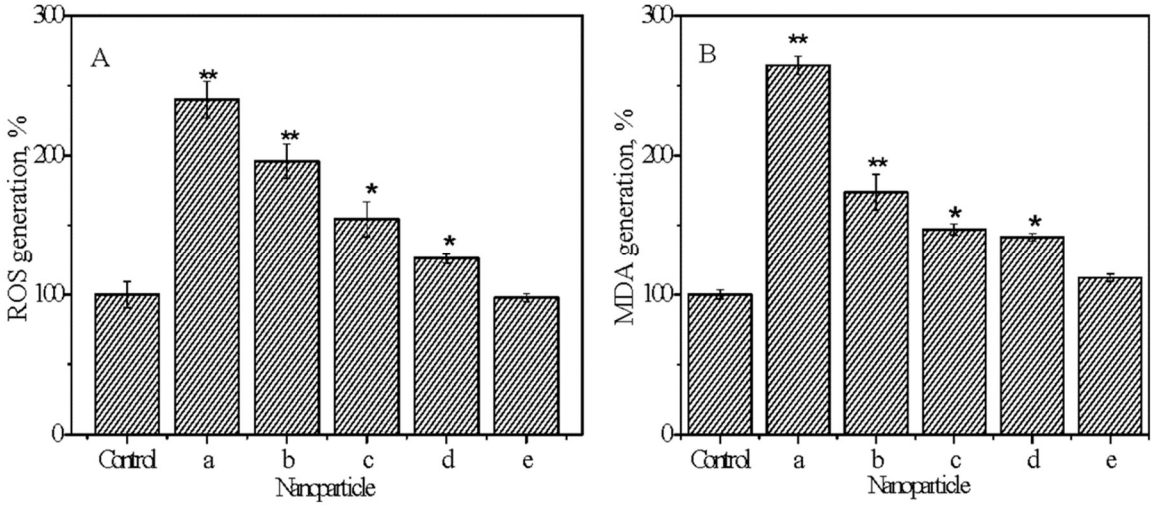

Figure 6.4. Production of ROS and MDA from titanium dioxide nanoparticles of different size and nature: a) 10 nm A; b) 25 nm A; c) 25 nm A/R; d) 50 nm A; e) 50 nm R, (A=anatase, R=rutile).[25]

Small particle size also increases cellular surface interaction, resulting in cell distortion, plasmolysis, cellular wall and/or membrane damage, thus easing the internalization of nanoparticles into the cell and ultimately resulting in cell damage or cell death.

Anda Gliga et al. (2014)[61] found that size-related nanoparticle toxicity mechanism influences cell viability regardless of the presence (or absence) of coating materials on the nanoparticles, while no evidence was found to confirm size-dependent genotoxicity during the same study. The study also inspected the relevance of the primary particle size compared to the size of the agglomerates: it was shown that primary particle size had the closest correlation to toxicity. However, contrasting results were obtained by Andersson (2011), who found that cell uptake can be quantitatively correlated to the agglomerates' size, rather than to the primary particle size. [62]

Particle size is also correlated to dissolution rate, through Noyes-Whitney equation[63]:

$$\frac{dm}{dt} = \frac{DA}{h}(C_s - C)$$

The dissolution rate (dissolved mass over time) is directly related to surface area A and to difference between current concentration and saturation concentration; therefore, the dissolution rate is proportionally higher if the area-to-mass ratio is higher. Moreover, particle size also influences solubility through Ostwald-Freundlich equation:

$$\frac{S}{S_0} = e^{\frac{2\gamma}{r}\cdot\frac{\bar{V}}{RT}}$$

As it can be seen, the smaller the radius (i.e., "r") is, the higher the solubility S becomes, being all the other variables state variables of the solution. Solubility is also physically influenced by surface morphology: in particular, by the level of aggregation, by the sphericity (less spherical particles present higher surface

tension), and again indirectly by particle size, since the lower the particle, the higher the surface tension on it. (Shao Wei Bian, 2011).[64]

Additionally, not only particle size influences the capability of a particle to disrupt the cellular membrane or its likelihood to be up taken by it. Nanoparticles, as well as every other ultrafine particle, present large specific surface area. A smaller particle size also means that the nanoparticle will have a higher specific surface area. Specific surface area is a derived physical measure obtained as the ratio between total surface area over total mass [L^2 M^{-1}]: therefore, decreasing the primary particle size, the specific surface area of a given mass is going to increase. Specific surface area is an important parameter in the quantification of surface-driven phenomena (i.e., adsorption, surface reaction, heterogeneous catalysis, etc.).

The contribution of specific surface area in the overall toxicity of ZnO and CuO nanoparticles was reviewed by Chang et al. (2012).[23] According to their findings, an increase in specific surface area does not only cause an enhancement of the accumulation potential of the particles, but also increases the specific chemical reactivity (reactivity per unit mass) and the interaction with biomolecules of the sample. An increased chemical reactivity makes nanoparticle more sensitive to solvents, resulting in an increased ion release in aqueous environment, which is a well-known toxic mechanism toward marine species. Likewise, increased surface area and chemical reactivity cause an increased production of superoxide radicals O2-, which will later form various species of ROS (reactive oxygen species).

While ROS are commonly produced in many natural processes and therefore are not toxic to many photosynthetic organisms themselves, an unbalanced amount of ROS will lead to a decrease in the ability of the targeted organism to repair the damage caused by oxidative stress.

A study from Singh et al. (2007)[65] highlighted how samples exposed to the same total surface area exhibited similar toxic responses, regardless of the differences in other parameters that are usually relevant in toxicological studies, such as concentration, total mass, primary particle size. This study made clear how

important specific surface area is in the overall toxicity of a sample, over other secondary parameters.

In the present study, the different nanoparticles were monitored by means of the ZS90 zetasizer, and their primary particle sizes were assessed to be 90 nm, 46 nm, and 70 nm for toothpaste-derived, sunscreen-derived and industrial TiO_2 nanoparticles, respectively. Throughout the experiment, their primary particle size changed respectively to 114 nm, 92 nm, and 81 nm. Given that the observed toxic effects were the highest for sunscreen-derived TiO_2 nanoparticles and the lowest for industrial TiO_2 nanoparticles, it looks like primary particle size and specific surface area did not play a key role in the toxic effects. Furthermore, measurements performed on SEM images are in agreement with the obtained results. This highlights surface adsorption as a key mechanism of toxicity for our experiment. Some mechanisms of cytotoxicity derived from surface adsorption are illustrated in Figure 6.5: as it can be seen, once adsorbed onto the cell's surface, the nanoparticle is phagocytized by a vesicle and, once inside the cell, it may cause several forms of damage such as protein damage, homeostatic changes or DNA damage, resulting in cell death.

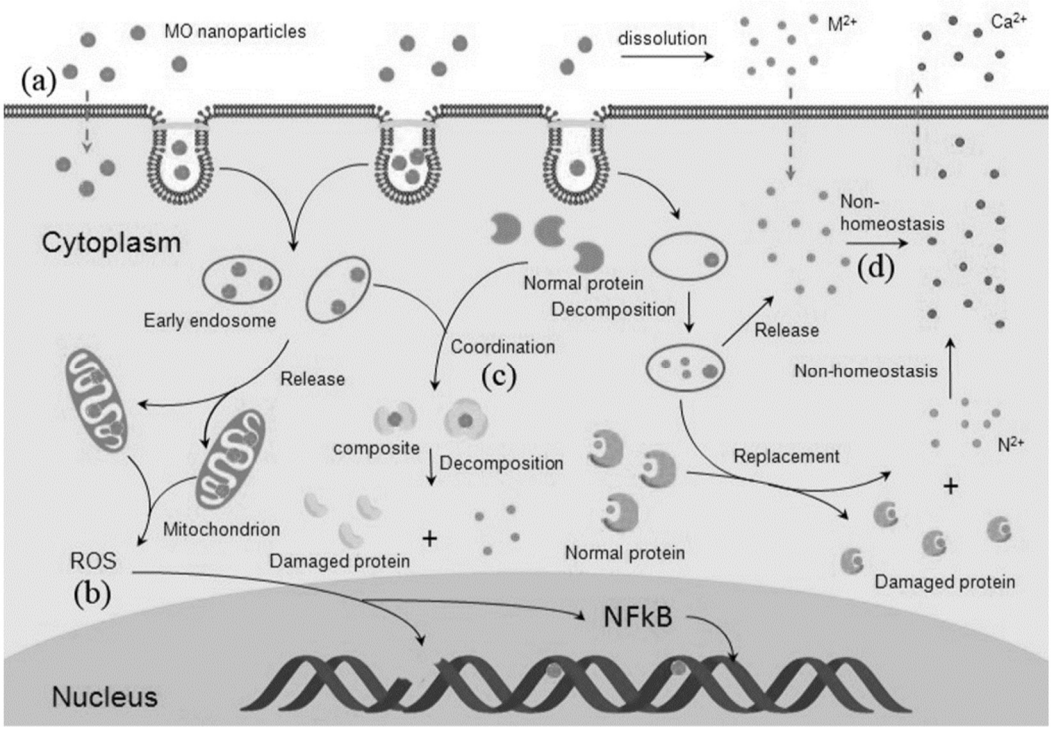

Figure 6.5. Several mechanisms of cytotoxicity caused by surface adsorption of nanoparticles.[23]

6.2.4 Concentration

Concentration has been largely inspected as a factor contributing to nanoparticles' toxicity towards many organisms, leading to different results. Dose-dependent toxicity was found in the present study, among the concentrations tested (1.0 mg/L, 2.5 mg/L, and 5.0 mg/L), for all of the tested nanoscale titania (industrial type, sunscreen-derived, and toothpaste-derived). However, results in literature are not always homogeneous regarding dose-dependent toxicity.

For instance, a study conducted by Naqvi et al. (2010)[66] showed that iron oxide NPs had no dose-dependent toxicity towards murine macrophage (J774) cells over an exposure period of 3 hours. However, a clear dependency of the toxicity on the concentration could be recorded after an incubation period of 6 hours. Therefore, concentration can not be solely addressed as a toxicity mechanism, yet its combination with other factors (either chemical, physical, biological, or environmental) can definitely result in toxic effects on many organisms.

In their study, for example, Naqvi et al. found that toxicity was ultimately due to apoptosis being caused by an induced ROS production, which itself was caused by oxidative stress due to the interaction between the nanoparticles and the cells.

In the present study, a similar result was obtained: in fact, before a well-defined break-through time, different TiO_2 NPs showed only slight differences in their toxic effects, while they became more remarkable after 72 hours of incubation. Looking at the measured data, a trend can be observed starting from 72h of incubation and increasing afterwards: this suggests a time-dependent toxicity mechanism, as toxicity only became visible after elapsing the aforementioned time interval. A possible mechanism that requires time in order to develop toxic effects is surface adsorption, followed by cytotoxic activities (i.e., membrane piercing and disruption, protein damage, homeostatic changes, and DNA damage). Being surface adsorption a potential key mechanism of toxicity for this case of study, nanoparticles' concentration still plays an important role as it increases the available surface per unit volume, thus increasing the toxic potential.

Figure 5.2 (see Section 5) shows the experimental results of the present study deriving from the concentration-dependent toxicity test, performed over 72h exposure time: as it can be seen, a consistent proportionality was found between the concentration of nanoparticles and the measured growth inhibition of *Thalassiosira pseudonana*. Despite the primary mechanism of toxicity requiring 72 hours of exposure was not explicitly investigated in the present study, it is warranted further research.

6.2.5 Photo-activity

Some engineered nanoparticles are well-known for their particular light-scattering capacity towards visible light. Titanium dioxide is, for instance, known to be the material with the highest opacity; however, when moving to the nanoscale, this metal oxide tends also to become photoactive, meaning that it shows an increased chemical reactivity and/or availability when exposed to UV radiation.

Photoactive behavior of TiO_2 NPs was studied by Brunet et al. (2009)[67], according to whose findings nano-TiO_2 tends to be more chemically reactive when exposed to UV radiation. However, the type of reactivity was influenced by the suspension medium: in fact, when suspended into pure water, TiO_2 NPs mainly produce hydroxide radicals, while they produced superoxide when suspended in MD (minimal Davis) medium. As a result, nano-TiO_2 was shown to be exclusively phototoxic, meaning that its toxic effects only affected the target organism (E. coli) under UV irradiation.

A study from Li et al. (2013)[68] emphasized how UV irradiation could influence the toxicity of nano-TiO_2 in a freshwater environment from a physical point of view. The target organism was a benthic amphipod (*Hyalella azteca*), and the experimental medium was LSW (Lake Superior water). The study highlighted how large aggregation and sedimentation could be observed when exposing the test sample to SSR (Simulated Solar Radiation) for 30 minutes, meaning that the tested TiO_2 NPs tend to aggregate and adsorb more easily when exposed to UV radiation.[68]

Experimental results showed a 21-fold difference in toxicity between samples tested under laboratory ambient light and samples exposed to SSR. However, the toxic mechanism related to surface attachment of nanoparticle remains not completely clear because many other factors influence it, and therefore needs to undergo further investigation. Figure 6.6 shows the amplification mechanisms due to UV irradiation towards TiO_2 nanoparticles-mediated toxicity in the environmental system of Lake Superior: in the upper layer of water, the risk of toxicity is mainly ascribed to UV irradiation, reacting with the suspended TiO_2 nanoparticles, producing ROS and harming the existing species by means of oxidative stress, while in le lowest layer, accumulation of aggregated nanoparticles occurs.

In the present study the samples were irradiated with UV light in 12h dark-light cycles. Despite no quantitative measurements of the effects of irradiation were taken, except for the UV lamp specifications (refer to Section 3.1.3), the experimental setup (use of Petri Dishes to perform toxicity tests) is shallow and

therefore UV irradiation remains a possible amplifier of the toxic effects exhibited by the different TiO_2 nanoparticles during this study.

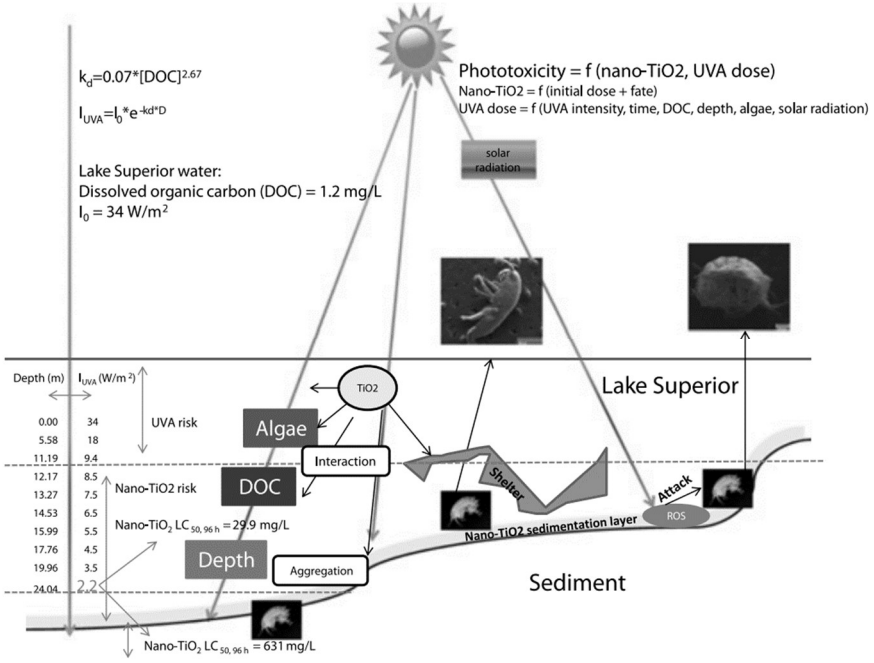

Figure 6.6. Interaction of UVA radiation with TiO_2 nanoparticles suspended and sedimented in Lake Superior.[68]

6.2.6 ROS Production and oxidative stress

As it was illustrated in the previous section, TiO_2 NPs are known to be extremely photoactive, which means that being exposed to UV radiation (including, but not limited to solar light) increases its their chemical reactivity and availability. One of the main products of the photo-induced chemical activity of TiO_2 NPs are ROS, (Reactive/Radical Oxygen Species).

The creation of said radicals occurs when TiO_2 (a semiconductor) is irradiated: if the radiation energy is higher than its band gap, electrons can be excited and therefore move to the conduction band, creating electron-holes.[69] If the electron vacancies are near to an aqueous interface, they can create many forms of radicals.

Other than from electronic excitation, ROS might also be produced from reactions occurring between NPs and specific biomolecules.

In fact, such radicals are naturally present in the aqueous environment in a low amount, and participate to a number of biochemical reactions, mostly acting as catalyzers for oxidative processes. However, an increased presence of ROS might induce oxidative stress in the cells, with multiple consequences.

A review article from Manke et al. (2013)[5] summarizes the "Mechanisms of Nanoparticle-Induced Oxidative Stress and Toxicity". According to their review, oxidative stress represents the micro-scale building block response for many known macroscopic pathologies/responses (e.g., fibrosis, inflammation, genotoxicity). The set of cellular pathologic responses to oxidative stress is shown in Figure 6.7.

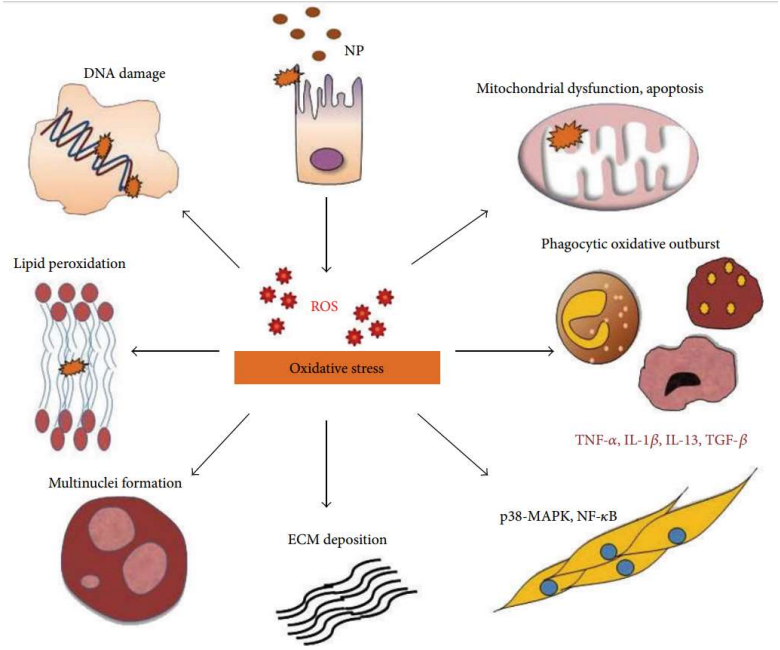

Figure 6.7. Pathologic responses to oxidative stess at the cellular level.[5]

Oxidative stress occurs at the cellular level when the production of ROS and the ability of the cell to either use or detoxify them become imbalanced. At lower levels of stress, response takes place only at the cellular level, with an increase in the production of antioxidants. If the level of ROS increases, the response extends to the tissue-level.[5]

Higher ROS production results in in mitochondrial damage and cell death. Moreover, an imbalanced amount of peroxide and free radicals results in damage to proteins and DNA, leading to genotoxicity. The review also summarized the effects of ROS production from nano-TiO_2, which are genotoxicity, cytotoxicity and apoptosis (induced cell death). Further knowledge needs to be gained regarding ROS production under UV irradiation from TiO_2 nanoparticles and, in particular, regarding the specific case of ROS production from TiO_2 contained in sunscreens or other personal care products: these products are highly likely to come in contact with UV radiation and therefore their photo-activity is warranted further study.

6.2.7 Crystal phase

The same nanoparticle, e.g., TiO_2 NP, can appear in various shapes, which are known as crystal phases. Different shapes depend on different environmental conditions during which the nanoparticle was formed including, but not limited to, the techniques used for the synthesis of the nanoparticle. Crystal phase not only makes a physical differentiation for the same nanoparticle, but also (in the case of nano-TiO_2) impacts the toxicity of the nanoparticle itself.

Four samples of nano-TiO_2 with different percentage compositions of anatase and rutile were tested by Suttiponparnit et al. (2011)[70] to understand their response to the environment. In order to isolate as much as possible the effects of the sole crystal phase, they performed their experiments at constant ionic strength.

Their results indicated that anatase-phase TiO_2 NPs had always the same IEP (iso-electric point, found at pH=4.8, slightly increasing with increasing percentages of anatase), while the IEP of rutile-type nano-TiO_2 was much lower, being it outside the tested range of pH (3 to 11). They justified this discrepancy with the fact that different nanoparticles were synthesized by means of different techniques and chemical procedures, likely influencing their behavior in aqueous environment.

The different eco-toxicological implications of the two crystalline phases of nano-TiO_2 have been inspected by Seitz et al. (2014)[71]. According to their findings,

100% anatase-TiO_2 NPs were up to four times more toxic than the 70% anatase-30% rutile nanoparticles, with respect to the target organism, Daphnia Magna.

Some possible factors causing this difference in toxicity were pointed out: firstly, anatase has a larger specific surface area, when compared to rutile nanoparticles of comparable particle size. Moreover, while the toxic mechanism of rutile-TiO_2 is mainly ROS production, anatase's toxicity also comes as a consequence of membrane leakage: while ROS production is a chemical toxic mechanism that can be impaired naturally (i.e. increased production of antioxidants), not much can be really done about the latter mechanism, making it more consistent in terms of toxicity.

Also, Jin et al. (2011)[72] showed that ROS production does not occur in the same way between the two crystal phases. In their experiments, they analyzed the in-vitro interaction between HaCaT cells (i.e., cell line established by human cells) and various TiO_2 NPs through X-ray absorption fine spectrometry, TEM imaging, and chemical precipitation method. Their results assessed that only anatase-form nano-TiO_2 has the appropriate surface properties to allow spontaneous ROS generation. Moreover, titanium (Ti) showed some interactions with proteins and DNA: although the release of Ti is not the most likely scenario, this raises the risk for secondary toxicity mechanisms that need to be inspected.

As for the nano-TiO_2 that was used for our experiments (commercially available, and derived from sunscreen and toothpaste), XRD analysis assessed that all of the three titanium nanopowders were anatase-phase TiO_2 NPs. Although the effect of crystal phase on the overall was not studied separately, the fact that all of the TiO_2 NPs were anatase-phase evens the situation, and we believe that the differences in toxicity are due to other parameters that vary between the tested TiO_2 nanoparticles. Nonetheless, further study should be devoted to understand the microscopic differences of the three samples and their toxicological implications.

6.3 Biological parameters

To this set belong those parameters that are not properties of the nanoparticle itself, but rather a property of the ecosystems that will be exposed to the nanoparticle. Knowing such properties, much more can be known about the fate of nanoparticles once they are up taken by living organisms from the environment, allowing to follow their path throughout the ecosystem and possibly draw a close cycle for them.

6.3.1 Bio-accumulation and bio-magnification

The marine diatom that was chosen as the target organism for our experiment, *Thalassiosira pseudonana*, belongs to the marine phytoplankton, and therefore makes the basement of the marine food pyramid. As it is well known, the food chain allows various phenomena of bio-accumulation and bio-magnification to happen; this means that if one basic organism uptakes a certain substance from the environment (e.g., toxic metals or other pollutants), the organism that follows the first one in the food chain will experience a magnification of the concentration of said contaminant, having eaten multiple basic organisms. Climbing the levels of the food pyramid, bio-magnification increases almost exponentially the concentration of the contaminant in the dominant organisms, causing the worst cases of accumulation in predators (humans, mammals, birds and fishes).

As it can be seen in Figure 6.8, bioaccumulation and biomagnification are two processes that happen simultaneously, being time the factor that allows accumulation, while magnification of the contaminant content takes place throughout species standing at different steps of the food pyramid. After time, and at the top of the food chain, dangerous concentrations of contaminants can be developed.

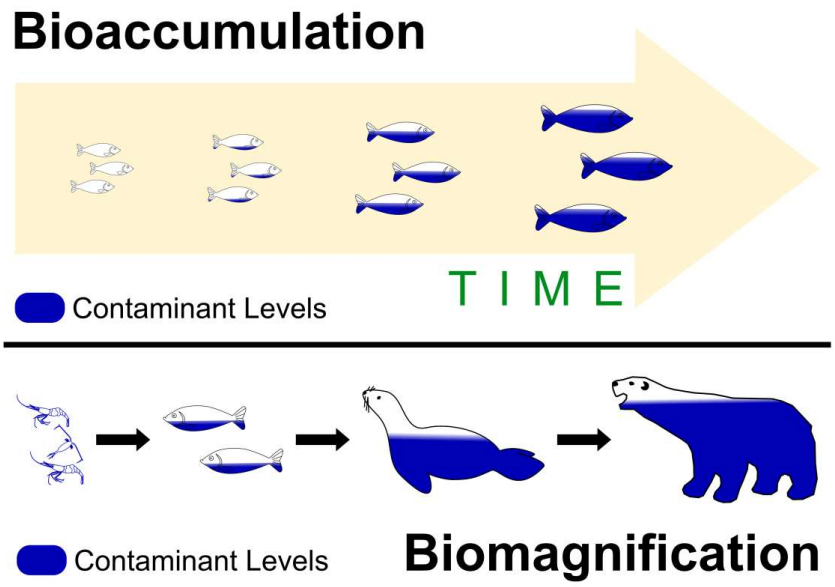

Figure 6.8. Bioaccumulation (time) and biomagnification across the food chain.(Image ©WWF)

Therefore, it is important to know the potential for bioaccumulation at the base of the food pyramid, in order to prevent these effects from scaling.

A study from Tan and Wang (2014)[73] investigates the modifications in the aqueous uptake of pollutants (Cadmium and Zinc) occurred in Daphnia Magna, upon exposure to nano-TiO_2.

As a result, the uptake capacity of the target organism increased greatly upon exposure to nano-TiO_2; then, after clearing it from the nano-TiO_2, the uptake rates went immediately back to the standard values. This result, together with observations on the levels of ROS, suggested that the increased uptake capacity was due to the increased number of available binding sites, which was provided by nano-TiO_2. This study can also be used to gain a better insight in our results and in their implications: SEM measurements revealed an increased particle size for TiO_2 NPs after exposing the marine diatoms to it. This might be due to the adsorption of some biomolecules on the available binding sites offered by TiO_2 NPs. If this is the case, further investigation has to be dedicated to the quantitative assessment of the uptake modification brought by exposure to TiO_2 NPs.

The literature survey that was performed, highlighted that the toxicity of TiO_2 nanoparticles can be influenced by a variety of factors, ranging from the physical and chemical properties of the particle, to some factors defined by the experimental environment's characteristics, to some biological traits of the targeted organism.

The literature survey pointed out some factors that are strongly recurrent in influencing nanoparticles-mediated toxicity, that can be recognized in the present case of study, such as:

Environmental Parameters

- pH and ionic strength of the culture medium,
- the light irradiation encouraging the photo-activity of the nanoparticles

Physical and Chemical Parameters

- the colloidal properties of the tested suspension,
- the electrochemical properties of the tested NPs (i.e., IEP),
- crystal phase of the nanoparticles,
- concentration and elapsed exposure time of the nanoparticles, and
- primary particle size.

Biological Parameters

- bioaccumulation,
- biomagnification.

The relevance of the aforementioned parameters was assessed both quantitatively by running specific growth inhibition tests and qualitatively, by comparing our initial data and results with the existing literature, allowing us to conclude the following:

- the likely high chloride content in our test medium (ASW) contributed to the reduction of the overall toxic effects,
- the measured values of pH make it unlikely for aggregation to occur, and therefore have not impacted toxicity significantly,

- the experiment was performed under 12h dark:light cycles, and UV irradiation is known to be a key factor for TiO_2 nanoparticles' toxicity,
- primary particle size was in most cases not small enough to be responsible of cell disruption, therefore it has likely contributed only marginally to the overall toxicity,
- a direct proportionality was found between the concentration of TiO_2 nanoparticles and the calculated growth inhibition, making concentration appear as a key toxicity factor in our study,
- different toxic behaviors were possible to observe on the tested samples after a break-through time equal to 72h, and a trend of direct proportionality between elapsed time and growth inhibition was observed after that time, and
- the anatase-phase TiO_2 of all the tested nanoparticles has likely enhanced the toxic effects in every experiment, however no significance can be ascribed to it, since all of the tested nanoparticles were of the same crystal phase.

The above list is also summarized in Table 6.1.

While every potential factor of the toxicity of nano-TiO_2 towards *Thalassiosira pseudonana* was deeply addressed in this survey, it was considered as the only variable parameter when analyzing it. This has been done for the sake of simplicity of the analysis, and to allow a better understanding of the mechanics involved in every parameter. However, it is easy to imagine that multiple parameters are likely to change simultaneously, showing synergistic and antagonistic effects one with each other. Such effects are still under deep research, and will be hopefully clarified in the future.

Table 6.1, Comparison of the toxicity factors observed in this study with other studies found in literature.

Toxicity Factor	Present case study			Other studies	Bibliography
	Industrial TiO_2	**Sunscreen TiO_2**	**Toothpaste TiO_2**	**Industrial TiO_2**	
ENVIRONMENTAL PARAMETERS					
Ionic Strength	Significant chloride content in our test medium (ASW) contributed to the reduction of the overall toxic effects	Significant chloride content in our test medium (ASW) contributed to the reduction of the overall toxic effects	Significant chloride content in our test medium (ASW) contributed to the reduction of the overall toxic effects	Increased ionic strength enhances aggregation and favors toxicity.	French et al. (2009)[50]
Environment pH	pH = 8.0 has likely impaired aggregation. Therefore, pH has not impacted toxicity significantly.	pH = 8.0 has likely impaired aggregation. Therefore, pH has not impacted toxicity significantly.	pH = 8.0 has likely impaired aggregation. Therefore, pH has not impacted toxicity significantly.	pH values above the IEP will impair aggregation and result in a lower aggregation and toxicity.	Lin et al. (2014)[25], Chambers et al. (2013)[51], Waalewijn - Kool et al. (2013)[52]
UV Irradiation / ROS Production	12h dark:light cycles performed. Anatase nano-TiO_2 is known to be photoactive under UV irradiation. Behavior is compatible with existing	12h dark:light cycles performed. Anatase nano-TiO_2 is known to be photoactive under UV irradiation. Behavior is compatible with existing	12h dark:light cycles performed. Anatase nano-TiO_2 is known to be photoactive under UV irradiation. Behavior is compatible with existing	Upon light irradiation (typically, UV), TiO_2 tends to be photo-active, with ROS production, consequent induced oxidative stress, resulting	Brunet et al. (2009)[67], Li et al. (2013)[68], Manke et al. (2013)[5]

	studies.	studies.	studies.	in increased toxicity.	
PHYSICAL and CHEMICAL PARAMETERS					
Particle Size and Specific Surface Area	Measured particle size of 10.5 nm by means of Scherrer equation. The finding is in contrast with the exhibited toxicity, suggesting that surface adsorption mechanisms might have had a more dominant role.	Measured particle size of 37.3 nm by means of Scherrer equation. The finding is in contrast with the exhibited toxicity, suggesting that surface adsorption mechanisms might have had a more dominant role.	Measured particle size of 6.1 nm by means of Scherrer equation. The finding is in contrast with the exhibited toxicity, suggesting that surface adsorption mechanisms might have had a more dominant role.	Particles lower than 22 nm in size can cause cell membrane disruption or can be up taken by cell nutrition.	Lin et al. (2014)[25], Andersson et al. (2011)[62]
Crystal Phase	The tested nanoparticle was assessed to be of anatase crystal phase. This has likely increased the toxic effects.	The tested nanoparticle was assessed to be of anatase crystal phase. This has likely increased the toxic effects.	The tested nanoparticle was assessed to be of anatase crystal phase. This has likely increased the toxic effects.	Anatase phase is reported to be the more potentially toxic than rutile phase, due to its structure, larger specific surface area, and natural photo-activity when	Lewicka et al. (2011)[3], Lewicka et al. (2012)[16], Suttiponparnit et al. (2011)[70], Seitz et al. (2014)[71], Jin et al. (2011)[72]

				exposed to UV radiation.	
Dose	TiO_2 dose was found to be directly proportional to growth inhibition within the tested range (1.0, 2.5, and 5.0 mg/L). Inhibition was lower than in products-derived nano-TiO_2.	TiO_2 dose was found to be directly proportional to growth inhibition within the tested range (1.0, 2.5, and 5.0 mg/L). Inhibition was the highest compared to the other two nano-TiO_2.	TiO_2 dose was found to be directly proportional to growth inhibition within the tested range (1.0, 2.5, and 5.0 mg/L). inhibition was lower than in sunscreen-derived nano-TiO_2.	Dose-dependent toxicity was found in many studies. However, thresholds for toxic effects are strongly influenced by target organism, light condition, crystal phase and other boundary conditions.	Lin et al. (2014)[25], Aruoja et al. (2009)[26], Miller et al. (2010)[74], Manzo et al. (2015)[75] Ahmad et al. (2013)[76]
Exposure Time	Significant differences in the toxic effects were observed after a break-through time of 72h. After said time, a direct relationship between time and toxicity can be observed.	Significant differences in the toxic effects were observed after a break-through time of 72h. After said time, a direct relationship between time and toxicity can be observed.	Significant differences in the toxic effects were observed after a break-through time of 72h. After said time, a direct relationship between time and toxicity can be observed.	Toxicity is always in direct relationship with exposure time. However, some mechan-isms act in really short timeframes (e.g., aggregation acts in t<1h), while some others require longer	Hartmann et al. (2012)[12], Aruoja et al. (2009)[26] French et al. (2009)[50], Manzo et al. (2015)[75], Ahmad et al. (2013)[76]

				exposure time (5 to 90 hours).	

Chapter 7 - Conclusions and future outlooks

The present study was aimed at the assessment of the toxic hazard posed by TiO_2 nanoparticles released in the marine environment. The choice of *Thalassiosira pseudonana* as the target organism for this study was driven by the fact that it is a really simple organism, yet contributing to the base level of the marine ecosystem and therefore holding capital importance.

Along with industrially-produced TiO_2 nanoparticles, this study wanted to shed some light on the properties and effects of TiO_2 nanoparticles derived (extracted) from commercial products, such as sunscreens and toothpastes. Therefore, TiO_2 nanoparticles of three different natures were used in this study: the industrial TiO_2 nanoparticles, acquired from Sigma-Aldrich, and the nanoparticles that were extracted from "Gardener's Armor" sunscreen and "Colgate" toothpaste, after buying them from a local store.

All of the experiments and procedures were performed at the Environmental Engineering Laboratory at the University of Miami.

The results of the present study highlighted some interesting trends. Firstly, a concentration dependent toxicity was exerted from all of the tested nanoparticles. Secondly it was found that growth inhibition caused by all of the tested titania is directly proportional to the exposure time, meaning that growth inhibition increases when the elapsed time increases. However, the most important finding of our study has been a solid evidence that puts the nature of the TiO_2 nanoparticles ahead of all of the other parameters, as a matter of growth inhibition: it was found that TiO_2 nanoparticles extracted from sunscreen had the most toxic effects on the selected organism, while the least toxic were the ones purchased by Sigma-Aldrich (thus being the toothpaste-derived in the middle). The quantitative influence shown by the nature of the nanoparticles surpassed the relationship with exposure time and concentration, opening great questions for the future.

Despite this work is somewhat unique in its genre, being one of the first studies to compare the toxic effects on marine species of TiO_2 nanoparticles of different

nature, the other results were encouragingly consistent with the existing literature. Since the available literature regarding this specific topic is currently scares, and having seen the outcome of this study, the subject is guaranteed further research and development in the future.

Although from the existing literature it might seem that the concentrations that have been tested in this study are unlikely to occur in nature, it has to be noted that this study also serves the purpose of modelling non-ordinary accumulation scenarios (point leak, sedimentation), giving a way to quantify their hazards toward the ecosystem.

Nonetheless, *Thalassiosira pseudonana* stays at the very base of the marine ecosystem and food chain: this means that bio-magnification phenomena might occur, and that major awareness is to be devoted to such important organisms (i.e., algae), that supply with oxygen the entire marine ecosystem.

Future developments and outlooks for the findings of this study are the investigation of the parameters that favored the toxicity of TiO_2 nanoparticles of a certain nature rather than another, therefore:

- dedicate more research activity to TiO_2 nanoparticles used in sunscreens: their coatings, other chemicals contained in sunscreen and investigate their interactions, especially in the very likely presence of UV radiation,
- Expand the current knowledge on the main toxicity mechanisms,
- Develop the knowledge necessary to implement newer industrial processes for consumer products, encouraging the use of less hazardous nanoparticles.

In general, much is still unknown in the field of nanoparticles, and further research is necessary. Possible hints on topics to develop are:

- Improvements in the use of certain nanoparticles (included TiO_2) as catalysts, using them for antibacterial purposes in medicine, filters, pharmaceuticals, etc.

- Development of realistic emission models for nanoparticles, that take into account the complex mechanics involved in their release, in order to provide a solid base for future studies,

Nanoparticles are a brand-new field in industry, and every day new applications for them are discovered. However, nowadays these new applications have outpaced the search for solution to the problem they pose.

It would be advisable, along with the ever-increasing number of new applications of nanomaterials, to adopt a sustainable approach to nanotechnologies, aiming research and development not only at new products and applications, but also at the solutions to the problems these innovations pose.

References

(1) Piccinno, F.; Gottschalk, F.; Seeger, S.; Nowack, B. Industrial production quantities and uses of ten engineered nanomaterials in Europe and the world. *J. Nanoparticle Res.* **2012**, *14* (9), 1–11.

(2) Robichaud, C. O.; Uyar, A. E.; Darby, M. R.; Zucker, L. G.; Wiesner, M. R. Estimates of upper bounds and trends in nano-TiO2 production as a basis for exposure assessment. *Environ. Sci. Technol.* **2009**, *43* (12), 4227–4233.

(3) Lewicka, Z. A.; Benedetto, A. F.; Benoit, D. N.; Yu, W. W.; Fortner, J. D.; Colvin, V. L. The structure, composition, and dimensions of TiO2 and ZnO nanomaterials in commercial sunscreens. *J. Nanoparticle Res.* **2011**, *13* (9), 3607–3617.

(4) Chang, X.; Zhang, Y.; Tang, M.; Wang, B. Health effects of exposure to nano-TiO 2 : a meta-analysis of experimental studies. *Nanoscale Res. Lett.* **2013**, *8* (51), 1–10.

(5) Manke, A.; Wang, L.; Rojanasakul, Y. Mechanisms of nanoparticle-induced oxidative stress and toxicity. *Biomed Res. Int.* **2013**, *2013*, 1–15.

(6) Sun, H.; Zhang, X.; Niu, Q.; Chen, Y.; Crittenden, J. C. Enhanced accumulation of arsenate in carp in the presence of titanium dioxide nanoparticles. *Water. Air. Soil Pollut.* **2007**, *178* (1-4), 245–254.

(7) Giraldo, A. L.; Peñuela, G. A.; Torres-Palma, R. A.; Pino, N. J.; Palominos, R. A.; Mansilla, H. D. Degradation of the antibiotic oxolinic acid by photocatalysis with TiO2 in suspension. *Water Res.* **2010**, *44* (18), 5158–5167.

(8) Savage, N.; Diallo, M. S. Nanomaterials and Water Purification: Opportunities and Challenges. *J. Nanoparticle Res.* **2005**, *7* (4-5), 331–342.

(9) Gupta, K.; Singh, R. P.; Pandey, A.; Pandey, A. Photocatalytic antibacterial performance of TiO $_2$ and Ag-doped TiO $_2$ against *S. aureus* . *P. aeruginosa* and *E. coli*. *Beilstein J. Nanotechnol.* **2013**, *4*, 345–351.

(10) Piskin, S.; Palantoken, A.; Sary Yilmaz, M. Antimicrobial Activity of. In *International Conference on Emerging Trends in Engineering and Technology (ICETET'2013)*; 2013; pp 91–94.

(11) Aitken, R. J.; Hankin, S. M.; Ross, B.; Tran, C. L.; Stone, V. *EMERGNANO : A review of completed and near completed environment , health and safety*

research on nanomaterials and nanotechnology; 2009.

(12) Hartmann, N. B.; Legros, S.; Von der Kammer, F.; Hofmann, T.; Baun, A. The potential of TiO2 nanoparticles as carriers for cadmium uptake in Lumbriculus variegatus and Daphnia magna. *Aquat. Toxicol.* **2012**, *118-119* (November), 1–8.

(13) Yin, T.; Gottschalk, F.; Hungerbühler, K.; Nowack, B. Comprehensive probabilistic modelling of environmental emissions of engineered nanomaterials. *Environ. Pollut.* **2014**, *185*, 69–76.

(14) Weir, A.; Westerhoff, P.; Fabricius, L.; Hristovski, K.; Goetz, N. Von. Titanium dioxide nanoparticles in food and personal care products. *Environ. Sci. Technol.* **2012**, No. 42, 2242–2250.

(15) Clément, L.; Hurel, C.; Marmier, N. Chemosphere Toxicity of TiO 2 nanoparticles to cladocerans , algae , rotifers and plants – Effects of size and crystalline structure. *Chemosphere* **2013**, *90*, 1083–1090.

(16) Lewicka, Z. A.; Yu, W. W.; Oliva, B. L.; Contreras, E. Q.; Colvin, V. L. Photochemical behavior of nanoscale TiO2 and ZnO sunscreen ingredients. *J. Photochem. Photobiol. A Chem.* **2013**, *263*, 24–33.

(17) Rincón, A.; Pulgarin, C. Bactericidal action of illuminated TiO 2 on pure Escherichia coli and natural bacterial consortia : post-irradiation events in the dark and assessment of the effective disinfection time. *Appl. Catal. B Environ.* **2004**, *49*, 99–112.

(18) Kwak, S. Y. and Kim, S. H. Hybrid organic/inorganic Reverse Osmosis (RO) membrane for preparation and characterization of TiO2 nanoparticle self-assembled aromatic polyamide membrane. *Environ. Sci. Technol.* **2001**, *35* (11), 2388–2394.

(19) Chen, Z.; Wang, Y.; Ba, T.; Li, Y.; Pu, J.; Chen, T.; Song, Y.; Gu, Y.; Qian, Q.; Yang, J.; et al. Genotoxic evaluation of titanium dioxide nanoparticles in vivo and in vitro. *Toxicol. Lett.* **2014**, *226*, 314–319.

(20) Minetto, D.; Libralato, G.; Ghirardini, A. V. Ecotoxicity of engineered TiO 2 nanoparticles to saltwater organisms : An overview. *Environ. Int.* **2014**, *66*, 18–27.

(21) Miller, R. J.; Bennett, S.; Keller, A. A.; Pease, S.; Lenihan, H. S. TiO2 nanoparticles are phototoxic to marine phytoplankton. *PLoS One* **2012**, *7* (1), 1–7.

(22) Bondarenko, O.; Ivask, A.; Kasemets, K.; Mortimer, M.; Kahru, A. Toxicity of Ag , CuO and ZnO nanoparticles to selected environmentally relevant test organisms and mammalian cells in vitro : a critical review. *Arch. Toxicol.* **2013**, 1181–1200.

(23) Chang, Y.; Zhang, M.; Xia, L.; Zhang, J.; Xing, G. The toxic effects and mechanisms of CuO and ZnO nanoparticles. *Materials (Basel).* **2012**, *5*, 2850–2871.

(24) OECD. *Oecd guidelines for the testing of chemicals*; 2011.

(25) Lin, X.; Li, J.; Ma, S.; Liu, G.; Yang, K.; Tong, M.; Lin, D. Toxicity of TiO2 nanoparticles to Escherichia coli: effects of particle size, crystal phase and water chemistry. *PLoS One* **2014**, *9* (10), e110247.

(26) Aruoja, V.; Dubourguier, H. C.; Kasemets, K.; Kahru, A. Toxicity of nanoparticles of CuO, ZnO and TiO2 to microalgae Pseudokirchneriella subcapitata. *Sci. Total Environ.* **2009**, *407* (4), 1461–1468.

(27) Burchardt, A. D.; Carvalho, R. N.; Valente, A.; Nativo, P.; Gilliland, D.; Garc, C. P.; Passarella, R.; Pedroni, V.; Lettieri, T. Effects of silver nanoparticles in diatom Thalassiosira pseudonana and Cyanobacterium Synechococcus sp. *Environ. Sci. Technol.* **2012**, No. 46, 11336–11344.

(28) Falciatore, A.; Bowler, C. Revealing the molecular secrets of marine diatoms. *Annu. Rev. Plant Biol.* **2002**, No. 29, 109–130.

(29) Armbrust, E. V.; Berges, J. A.; Bowler, C.; Green, B. R.; Martinez, D.; Putnam, N. H.; Zhou, S.; Allen, A. E.; Apt, K. E.; Bechner, M.; et al. The genome of the diatom Thalassiosira pseudonana: ecology, evolution, and metabolism. *Science (80-.).* **2004**, *306* (October), 79–85.

(30) EPA. *State of the science literature review : nano titanium dioxide*; 2010.

(31) Bhatta, H.; Enderlein, J.; Rosengarten, G. Fluorescence Correlation Spectroscopy to study diffusion through diatom nanopores. *J. Nanosci. Nanotechnol.* **2009**, *9*, 6760–6766.

(32) Research & Discovery | Clinical Diagnostics - Beckman Coulter, Inc.

(33) Zetasizer Nano ZS90 for particle size and zeta potential measurements.

(34) HappyLight Liberty 5K Natural Spectrum Energy Lamp.

(35) Thermo Scientific Orion 720Aplus and 920Aplus pH/mV/ISE Benchtop

Meters:Thermometers,.

(36) FAO. *Manual on the production and use of live food for aquaculture*; 1996.

(37) Guillard, R. R. L.; Ryther, J. H. Studies of marine planktonic diatoms: I. cyclotella nana hustedt, and Detonula confervacea (cleve) gran. *Can. J. Microbiol.* **1962**, *8* (2), 229–239.

(38) Keller, M. D.; Seluin, R. C.; Claus, W.; Guillard, R. R. L.; Provasoli, L.; Pinter, I. J. Media for the culture of oceanic ultraphytoplankton. *Deep Sea Res. Part B. Oceanogr. Lit. Rev.* **1988**, *35* (6), 561.

(39) Sigma Aldrich. Product Specification - Titanium(IV) oxide, anatase nanopowder, <25 nm particle size, 99.7% trace metals basis. p 63103.

(40) CCMP1335 | NCMA - Culturing Diversity.

(41) Sobrino, C.; Ward, M. L.; Neale, P. J. Acclimation to elevated carbon dioxide and ultraviolet radiation in the diatom Thalassiosira pseudonana : Effects on growth , photosynthesis , and spectral sensitivity of photoinhibition. *Limonology Oceanogr.* **2008**, *53* (2), 494–505.

(42) Davis, A. K.; Hildebrand, M.; Palenik, B. Gene expression induced by copper stress in the diatom Thalassiosira pseudonana. *Eukaryot. Cell* **2006**, *5* (7), 1157–1168.

(43) Atif, M.; Farooq, W. A.; Fatehmulla, A.; Aslam, M.; Ali, S. M. Photovoltaic and impedance spectroscopy study of screen-printed TiO2 based CdS quantum dot sensitized solar cells. *Materials (Basel).* **2015**, No. 8, 355–367.

(44) Ingale, S. V; Wagh, P. B.; Tripathi, A. K.; Srivastav, R.; Singh, I. K.; Bindal, R. C.; Gupta, S. C. TiO 2 — Polysulfone beads for use in photo oxidation of Rhodamine B. *Soft Nanosci. Lett.* **2012**, *2* (October), 67–70.

(45) Cao, P.; Cai, X.; Lu, W.; Zhou, F.; Huo, J. Growth inhibition and induction of apoptosis in SHG-44 Glioma cells by chinese medicine formula “Pingliu Keli.” *Evid. Based. Complement. Alternat. Med.* **2011**, 1–9.

(46) Cunningham, A. B.; Lennox, J. E.; Ross, R. J. Typical Growth Curve http://www.hypertextbookshop.com/biofilmbook/v004/r003/.

(47) Barker, P. J.; Branch, A. The interaction of modern sunscreen formulations with surface coatings. *Prog. Org. Coatings* **2008**, *62* (April), 313–320.

(48) Loosli, F.; Le Coustumer, P.; Stoll, S. TiO2 Nanoparticles Aggregation and

Disaggregation in Presence of Alginates and Humic Acids : pH and Concentration Effects on Suspension Stability. **2013**

(49) Keller, A. A.; Wang, H.; Zhou, D.; Miller, R. J. Stability and Aggregation of Metal Oxide Nanoparticles in Natural Aqueous Matrices Stability and Aggregation of Metal Oxide Nanoparticles in Natural Aqueous Matrices. **2010**, No. June 2016.

(50) French, R.; Jacobson, A. R.; Penn, R. L.; Baveye, P.; French, R. A. Influence of ionic strength , pH , and cation calence on aggregation kinetics of titanium dioxide nanoparticles. *Environ. Sci. Technol.* **2009**, *43* (April), 1354–1359.

(51) Chambers, B. A.; Nabiool, A. A. R. M.; Bae, S.; Nirupam, A.; Katz, L.; B., N. S.; Krisitis, M. J. Effects of chloride and ionic strength on physical morphology, dissolution, and bacterial toxicity of silver nanoparticles. *Environ. Sci. Technol.* **2013**.

(52) Waalewijn-Kool, P.; Ortiz, M.; Lofts, S.; van Gestel, C. The effect of pH on the toxicity of zinc oxide nanoparticles to Folsomia candida in amended field Soil. *Environ. Toxicol. Chem.* **2013**, *32* (10), 2349–2355.

(53) Seitz, F.; Koblenz-landau, U.; Rosenfeldt, R. R.; Koblenz-landau, U. Effects of silver nanoparticle properties , media pH and dissolved organic matter on toxicity to Daphnia magna. *Ecotoxicol. Environ. Saf.* **2015**, No. January, 263–270.

(54) Hund-Rinke, K.; Schlich, K.; Wenzel, A. TiO2 nanoparticles - Relationship between dispersion preparation method and ecotoxicity in the algal growth test. *Umweltwissenschaften und Schadstoff-forsch.* **2010**, *22* (November), 517–528.

(55) Verdier, T.; Coutand, M.; Bertron, A.; Roques, C. Antibacterial activity of TiO2 photocatalyst alone or in coatings on E. coli: the influence of methodological aspects. *Coatings* **2014**, 670–686.

(56) Chen, K. L.; Smith, B. A.; Ball, W. P.; Fairbrother, D. H. Assessing the colloidal properties of engineered nanoparticles in water : case studies from fullerene C 60 nanoparticles and carbon nanotubes. *Environ. Chem.* **2010**, No. 7, 10–27.

(57) Patil, S.; Sandberg, A.; Heckert, E.; Self, W.; Seal, S. Protein adsorption and cellular uptake of cerium oxide nanoparticles as a function of zeta potential. *Biomaterials* **2007**, *28* (31), 4600–4607.

(58) Schwegmann, H.; Feitz, A. J.; Frimmel, F. H. Influence of the zeta potential on the sorption and toxicity of iron oxide nanoparticles on S . cerevisiae and E . coli. *J. Colloid Interface Sci.* **2010**, *347* (1), 43–48.

(59) Roiter, Y.; Ornatska, M.; Rammohan, A. R.; Balakrishnan, J.; Heine, D. R.; Minko, S. Interaction of nanoparticles with lipid membrane. *Nano Lett.* **2008**, *8* (3), 941–944.

(60) Wilhelm, C.; Billotey, C.; Roger, J.; Pons, J. N.; Bacri, J.; Gazeau, F. Intracellular uptake of anionic superparamagnetic nanoparticles as a function of their surface coating. *Biomaterials* **2003**, *24*, 1001–1011.

(61) Gliga, A. R.; Skoglund, S.; Wallinder, I. O.; Fadeel, B.; Karlsson, H. L. Size-dependent cytotoxicity of silver nanoparticles in human lung cells: the role of cellular uptake , agglomeration and Ag release. *Part. Fibre Toxicol.* **2014**, *11* (11), 1–17.

(62) Andersson, P. O.; Lejon, C.; Ekstrand-hammarström, B. Polymorph- and size-dependent uptake and toxicity of TiO2 nanoparticles in living lung epithelial cells. *Small* **2011**, No. 4, 514–523.

(63) Dokoumetzidis, A.; Macheras, P. A century of dissolution research : from Noyes and Whitney to the Biopharmaceutics Classification System. *Int. J. Pharm.* **2006**, *321*, 1–11.

(64) Bian, S.; Mudunkotuwa, I. A.; Rupasinghe, T.; Grassian, V. H. Aggregation and dissolution of 4 nm ZnO nanoparticles in aqueous environments : influence of pH, ionic strength, size, and adsorption of Humic Acid. *Langmuir* **2011**, No. February, 6059–6068.

(65) Singh, S.; Shi, T.; Duffin, R.; Albrecht, C.; Berlo, D. Van; Höhr, D.; Fubini, B.; Martra, G.; Fenoglio, I. Endocytosis, oxidative stress and IL-8 expression in human lung epithelial cells upon treatment with fine and ultrafine TiO 2 : role of the specific surface area and of surface methylation of the particles. *Toxicol. Appl. Pharmacol.* **2007**, *222* (2), 141–151.

(66) Naqvi, S.; Samim, M.; Abdin, M.; Ahmed, F. J.; Maitra, A.; Prashant, C.; Dinda, A. K. Concentration-dependent toxicity of iron oxide nanoparticles mediated by increased oxidative stress. *Int. J. Nanomedicine* **2010**, 983–989.

(67) Brunet, N. A.; Lyon, D. Y.; Alvarez, P. J. J. Comparative photoactivity and antibacterial properties of C 60 fullerenes and titanium dioxide nanoparticles. *Environ. Sci. Technol.* **2009**, *43* (12), 4355–4360.

(68) Li, S.; Ma, H.; Diamond, S. A. Phototoxicity of TiO2 nanoparticles to a freshwater benthic amphipod : are benthic systems at risk? *Sci. Total Environ.* **2014**, *466-467* (January), 800–808.

(69) Fujishima, A.; Honda, K. Electrochemical photolysis of water at a semiconductor electrode. *Nature* **1972**, *238*, 37–38.

(70) Suttiponparnit, K.; Jiang, J.; Sahu, M.; Suvachittanont, S. Role of surface area, primary particle size, and crystal phase on titanium dioxide nanoparticle dispersion properties. *Nanoscale Res. Lett.* **2011**, *6* (27), 1–8.

(71) Seitz, F.; Koblenz-landau, U.; Rosenfeldt, R. R.; Koblenz-landau, U. Size- , surface- and crystalline structure composition-related effects of titanium dioxide nanoparticles during their aquatic life cycle. *Sci. Total Environ.* **2014**, No. 493, 891–897.

(72) Jin, C.; Tang, Y.; Yang, F. G.; Li, X. L. Cellular toxicity of TiO2 nanoparticles in anatase and rutile crystal phase. *Biol. Trace Elem. Res.* **2011**, *141* (1), 3–15.

(73) Tan, C.; Wang, W. Modification of metal bioaccumulation and toxicity in Daphnia magna by titanium dioxide nanoparticles. *Environ. Pollut.* **2014**, *186*, 36–42.

(74) Miller, R. J.; Lenihan, H. S.; Muller, E. B.; Tseng, N.; Hanna, S. K.; Keller, A. A. Impacts of metal oxide nanoparticles on marine phytoplankton. *Environ. Sci. Technol.* **2010**, *44* (19), 7329–7334.

(75) Manzo, S.; Buono, S.; Rametta, G.; Miglietta, M.; Schiavo, S.; Di Francia, G. The diverse toxic effect of SiO2 and TiO2 nanoparticles toward the marine microalgae Dunaliella tertiolecta. *Environ. Sci. Pollut. Res.* **2015**, 15941–15951.

(76) Ahmad, R.; Meryam, S. TiO 2 nanoparticles as an antibacterial agents against E. coli. *Int. J. Innov. Res. Sci. Eng. Technol.* **2013**, *2* (8), 3569–3574.

ACKNOWLEDGMENTS

First of all, I want to deeply thank Professor Andrea Bolognesi, for his great patience in helping my study experience throughout this year, regardless of every limitation of time and distance.

I wish to thank Seok-Ju Seo, for sharing his practical and scientific knowledge with me, helping to set up the experimental part of this work.

I really want to thank my whole family, and my girlfriend Ilaria, for their continuous support and input to get the maximum from my experience at the University of Miami this year, as well as during the past four years, not just to gain the best from my studies, but also, and most importantly, to set these years as a major milestone of my life.

I want to thank Eleonora Spisni, Riccardo Baricci, Yara Wehbe, Matthew Young, Maria Arguelles, Crystal Léon, Ana Dvorak, and Kusumitha Perera for being extremely valuable classmates, but most importantly great friends.

I want to acknowledge some of my friends that accompanied me in this experience: Barbara, Vincenzo, Caterina, Alberto, Anna, Maria Rita, Camilla and Luigi as well as every other friend that has had a good thought for me during this time.